Upper Ocean Water Properties and Currents along Paired Sections in the Northern California Current, September 1999-2003

Jane H. Fleischbein
Adriana Huyer
P. Michael Kosro
Robert L. Smith
Jennifer J. Wetz
and
Patricia A. Wheeler

College of Oceanic and Atmospheric Sciences
Oregon State University
Corvallis OR 97331-5003

Data Report 204
Reference 2006-1
January 2006

Table of Contents

List of Tables and Figures

Figure 13. Upper-ocean distributions of fluorescence voltage (V). Contours: dashed at 0.5 V; thin at 1, 3; heavy at 2, 4; full scale is at 15 V in 2002 and at 5.0 V in other years. Fluorometer calibration is believed to remain about the same within each cruise though it may vary from cruise to cruise.

Figure 14. Upper-ocean distributions of total nitrate (μmol/l).

Figure 15. Upper-ocean distributions of phosphate (μmol/l).

Figure 16. Upper-ocean distributions of silicate (μmol/l).

Figure 17. Upper-ocean distributions of chlorophyll (mg/m^3). Contours are at 0.5 (dashed), 1, and 2, 4, 8 (heavy), 12 and 16 mg/m^3.

Figure 18. Offshore profiles of surface temperature and salinity.

Figure 19. Offshore profiles of steric height (J/kg) of the sea surface relative to 150 dbar and 500 dbar.

Figure 20. Offshore profiles of surface density and of surface mixed layer depth, defined as the depth at which potential density exceeds the surface value by 0.01 kg m^{-3}.

Figure 21. Offshore profiles of surface density and of surface mixed layer depth, defined as the depth at which potential density exceeds the surface value by 0.1 kg m^{-3}.

Figure 22. T-S characteristics of all CTD stations. Shelf stations are plotted in red.

Figure 23. Superimposed groups of T-S characteristics. Upper row: NH (black) on CR (red). Lower row: CR (red) on NH (black).

Figure 24. Detail of T-S characteristics in the permanent halocline. Shelf stations are plotted in red.

Figure 25. Oxygen-salinity characteristics of all CTD stations. Shelf stations are plotted in red.

Figure 26. Detail of oxygen-salinity characteristics in and below the permanent halocline. Shelf stations are plotted in red.

Figure 27. Nitrate-phosphate relations for all rosette samples. Shelf stations are plotted in red.

Figure 28. Silicate-phosphate relations for all rosette samples. Shelf stations are plotted in red.

Figure 29. Nitrate-salinity relations. Shelf stations are plotted in red.

Figure 30. Nitrate-salinity relations for samples with salinities $\geq$ 32 psu. Shelf stations are plotted in red.

Figure 31. Nitrate-salinity relations for samples with salinities $\geq$ 32 psu: CR data (red) superimposed on NH data (black).

Figure 32. Phosphate-salinity relations. Shelf stations are plotted in red.

Figure 33. Phosphate-salinity relations for samples with salinities ≥ 32 psu. Shelf stations are plotted in red.

Figure 34. Phosphate-salinity relations for samples with salinities ≥ 32 psu: CR data (red) superimposed on NH data (black).

Figure 35. Silicate-salinity relations. Shelf stations are plotted in red.

Figure 36. Silicate-salinity relations for samples with salinities ≥ 32 psu. Shelf stations are plotted in red.

Figure 37. Silicate-salinity relations for rosette samples with salinities ≥ 32 psu: CR data (red) superimposed on NH data (black).

Upper Ocean Water Properties and Currents along Paired Sections in the Northern California Current, September 1999-2003

Introduction

As part of the U. S. GLOBEC NorthEast Pacific Program we made repeated seasonal hydrographic surveys in the northern California Current system (Figure 1) between July 1997 and September 2003. These surveys included sampling along a pair of hydrographic sections, one north (at 44.6ºN) and one south (at 41.9ºN) of Cape Blanco (Figure 1) in September of five years (1999-2003). The coastal upwelling associated with the California Current experiences maximum upwelling during summer, and usually continues through much of September; upwelling is usually stronger at 42ºN than at 45ºN (Figure 2). One purpose of this report is to show differences and similarities between the coastal upwelling domains north and south of Cape Blanco. We present graphical summaries of the physical oceanographic and biochemical observations along both sections, principally in the form of zonal sections (0-160 km from shore, 0-150 m depth). We also show offshore profiles of a few selected properties, and some characteristic diagrams (T-S, oxygen-S, etc.). Similar reports showing results for mid-summer and for spring have already been published (Fleischbein *et al.*, 2005a, b).

Sampling

The NH-line at 44.6ºN off Newport, Oregon, lies about 130 km south of the mouth of the Columbia River, and spans a relatively wide shelf. This line was sampled seasonally from 1961 to 1971 (Smith *et al.*, 2001), and then sporadically until July 1997 when GLOBEC resumed sampling of the NH-line until the fall of 2003. The NH-line consists of 12 CTD stations whose separation increases with distance from shore; the most offshore station, NH-85, is at 126.05ºW, 157 km from shore.

The CR-line at 41.9ºN off Crescent City, California, lies 300 km farther south and spans a narrower shelf; this line was originally sampled during the 1981-1984 SuperCODE experiment (Huyer *et al.*, 2002). The CR-line originally consisted of nine CTD stations with the most offshore at 125.3ºW. This section was extended in 2000 by adding two stations (at 125.7ºW and 126.0ºW). Beginning in September 2000, the station CR-9 at 125.3ºW was dropped in favor of CR-9a at 125.4ºW.

Sampling along both sections included CTD/rosette casts at standard stations (Table 1), and continuous operation of an Acoustic Doppler Current Profiler; results of the concurrent zooplankton sampling are not included in this report.

Details of CTD data collection, calibration and processing are available in a series of data reports (Fleischbein *et al.*, 1999; 2001; 2002; 2003). Accuracy of the processed data is estimated to be better than ±0.01ºC for temperature, ±0.003 psu for salinity, ±1 dbar for pressure, and ±0.2 ml/l for dissolved oxygen. A SeaTech fluorometer was also mounted on the CTD/rosette frame.

Biochemical sampling was conducted at most stations (Table 1). Water samples from the upper 150 m were analyzed to determine concentrations of inorganic nutrients (nitrate, phosphate, silicate, nitrite, ammonium), phytoplankton biomass (chlorophyll-*a*), particulate organic carbon and nitrogen, and dissolved organic carbon and nitrogen. Samples were collected with 5-L Niskin bottles on a 12-bottle rosette, with samples

taken at about 150 m, 100 m, and at 10 m intervals in the upper 70 m. Analytical methods have been described by Corwith and Wheeler (2002) and by Hill and Wheeler (2002). The following plots in this data report include only nutrient and chl-*a* data. Sampling protocols, analytical information and tabulated values of nutrient and chl-*a* are available in the data report by Wetz et al. (2004).

Upper-ocean currents were measured along each section by a shipborne acoustic Doppler current profiler (ADCP). On most cruises the ADCP system was narrowband, 150 kHz, with 8-m bins, manufactured by RD Instruments. ADCP data were collected in 2.5 min ensembles and processed using the University of Hawaii CODAS system (Firing, Ranada and Caldwell, 1995). Profiles were screened manually for bottom interference, corrected for gyrocompass errors with data from an Ashtech 3DF GPS-based system, calibrated for transducer and gyrocompass alignment, and processed to absolute currents by referring to differential GPS data. Kosro (2002) estimates high-frequency noise (due to tides and inertial currents) to be about ±8 cm/s.

Vertical Distributions

The upper-ocean distributions (surface to 150 m depth) are shown for fifteen parameters: temperature, salinity, potential density, geostrophic velocity (relative to both 150 dbar and 500 dbar), ADCP measured current (northward and eastward components), buoyancy frequency, spiciness, dissolved oxygen saturation, fluorescence voltage, nitrate, phosphate, silicate, and chlorophyll (Figures 3-17). For each parameter, distributions are shown for both sections in each fall.

Offshore Profiles

Offshore profiles (Figure 18-21) are shown for a few selected parameters: surface temperature and salinity, steric height, and mixed layer depth (determined from two separate criteria).

Characteristic Diagrams

T-S diagrams (Figures 22-24) include all available data, i.e., from depths below 150 m (to 1000 m) as well as above 150 m. To facilitate comparison and interpretation, we show the T-S diagrams superimposed as well as separately. We also show oxygen-salinity (Figures 25-26), nutrient-phosphate (Figures 27-28) and nutrient-salinity diagrams (Figures 29-37).

For most characteristic diagrams, we distinguish from "shelf" data (NH-1 to NH-15 and CR-1 to CR-3) from offshore data (all remaining stations). For some T-S and nutrient-salinity relations we show two versions: one with a wide salinity range (30-35 psu), and one with a narrow salinity range (32 to 34.5 psu).

Acknowledgements

We are grateful to all those who participated in collecting these data, including the captain, crew and especially the marine technicians of R/V Wecoma and R/V New Horizon. We are supported by the National Science Foundation through Grant OCE 0000733 and OCE 0434810. The LTOP hydrographic data collection and analysis are supported by the U.S. GLOBEC NorthEast Pacific Program, funded jointly by NSF and NOAA.

References

Corwith, H.L. and P.A. Wheeler. 2002. El Niño related variations in nutrient and chlorophyll distributions off Oregon. *Progr. Oceanogr.*, **54**, 361-380.

Firing, E., J. Ranada and P. Caldwell. 1995. *Processing ADCP data with the CODAS software system, version 3.1.* Honolulu, HI: University of Hawaii.

Flament, P. 2002. A state variable for characterizing water masses and their diffusive stability: spiciness. *Progress in Oceanography*, **54**, 491-500.

Fleischbein, J., A. Huyer, P. M. Kosro, R. L. Smith and P. A. Wheeler. 2005a. Upper ocean water properties and currents along paired sections in the northern California Current, summer 1998-2003. College of Oceanic and Atmospheric Sciences, Oregon State University, *Data Report 201*, Ref. 2005-4, 41 pp.

Fleischbein, J.H., A. Huyer, P. M. Kosro, R. L. Smith, J. J. Wetz, and P. A. Wheeler. 2005b. Upper ocean water properties and currents along paired sections in the northern California Current, spring 1998-2003. College of Oceanic and Atmospheric Sciences, Oregon State University, *Data Report 203*, Ref. 2005-6, 42 pp.

Fleischbein, J., J. Hill, A. Huyer, R. L. Smith and P. A. Wheeler. 1999. Hydrographic data from the GLOBEC long-term observation program off Oregon, 1997 and 1998. College of Oceanic and Atmospheric Sciences, Oregon State University, *Data Report 172*, Ref. 99-1, 288 pp.

Fleischbein, J., A. Huyer, and R. L. Smith, 2001. Hydrographic data from the GLOBEC long-term observation program off Oregon, 1999 and 2000. College of Oceanic and Atmospheric Sciences, Oregon State University, *Data Report 183*, Ref. 2001-3, 290 pp.

Fleischbein, J., A. Huyer, and R. L. Smith, 2002. Hydrographic data from the GLOBEC long-term observation program off Oregon, 2001. College of Oceanic and Atmospheric Sciences, Oregon State University, *Data Report 187*, Ref. 2002-3, 168 pp.

Fleischbein, J., A. Huyer, and R. L. Smith, 2003. Hydrographic data from the GLOBEC long-term observation program off Oregon, 2002 and 2003. College of Oceanic and Atmospheric Sciences, Oregon State University, *Data Report 192*, Ref. 2003-2, 296 pp.

Hill, J.K. and P.A. Wheeler. 2002. Organic carbon and nitrogen in the northern California Current system during July 1997: comparison of offshore, river plume, and coastally upwelled water. *Progr. Oceanogr.*, **53**, 369-387.

Kosro, P. M. 2002. A poleward jet and an equatorward undercurrent observed off Oregon and northern California during the 1997-98 El Niño, *Progr. Oceanogr.*, **54**, 343-360.

Reid, J. L., and A. W. Mantyla, 1976. The effect of geostrophic flow upon coastal sea elevations in the northern North Pacific Ocean. *J. Geophys. Res.,* **81**, 3100-3110.

Smith, R. L., A. Huyer and J. Fleischbein. 2001. The coastal ocean off Oregon from 1961 to 2000: Is there evidence of climate change or only of Los Niños? *Progr. Oceanography, 49*, 63-93.

Wetz, J. J., J. Hill, H. Corwith and P. A. Wheeler. 2004. Nutrient and extracted chlorophyll data from the GLOBEC Long-Term Observation Program, 1997-2004. *Data Report 193*, COAS Ref. 2004-1, 135 pp.

Table 1. CTD and biochemical (BC) sampling along paired NH- and CR-Lines, September 1999 to 2003.

		22-25 Sept 1999			7-10 Sept 2000			4-9 Sept 2001			28 Sept -1 Oct 2002			26-29 Sept 2003		
		Stn No	Max Depth	BC	Stn No	Max Depth	BC	Stn No	Max Depth	BC	Stn No	Max Depth	BC	Stn No	Max Depth	BC
NH-1	-124.100	1	20		1	24		1	25					1	26	
NH-3	-124.130	2	46		2	43		2	44		1	41		2	44	
NH-5	-124.177	3	57	x	3	52	x	3	56	x	2	53	x	3	55	x
NH-10	-124.295	4	76		4	76		4	78		3	74		4	77	
NH-15	-124.412	5	86	x	5	90	x	5	88	x	4	87	x	5	87	x
NH-20	-124.528	6	136		6	139		6	138		5	134		6	136	
NH-25	-124.650	7	285	x	7	280	x	7	281	x	6	272	x	7	280	x
NH-35	-124.883	8	426	x	8	430	x	8	426	x	7	435	x	9	430	x
NH-45	-125.117	9	694	x	9	680	x	9	696	x	8	684	x	10	680	x
NH-55	-125.367	10	1008		10	1006		10	1005		9	1005		11	1005	
NH-65	-125.600	11	1008	x	11	1005	x	11	1006	x	10	1006	x	12	1006	x
NH-85	-126.050	12	1008	x	12	1007	x	12	1005	x	12	1014	x	13	1006	x
CR-1	-124.300	21	35	x	21	35	x	21	36	x	19	35	x	14	35	x
CR-2	-124.400	22	61		22	64		22	62		20	63		15	62	
CR-3	-124.500	23	127	x	23	130	x	23	130	x	21	132	x	16	130	x
CR-4	-124.600	24	496	x	24	500	x	24	505	x	22	495	x	17	500	x
CR-5	-124.700	25	655	x	25	651	x	25	630	x	23	646	x	18	650	x
CR-6	-124.800	26	688		26	686		26	692		18	689		19	691	
CR-7	-125.000	27	826	x	27	811	x	27	838	x	17	802	x	20	811	x
CR-8	-125.200	28	1006		28	1006		28	1006		16	1005		21	1005	
CR-9	-125.333	29	1005	x	29	1007	x									
CR-9a	-125.400							29	1005	x	15	1002	x	22	1005	x
CR-10	-125.667				30	1006		30	1006	x	14	1007		23	1005	
CR-11	-126.000				31	1005	x				13	1006	x	24	1005	x

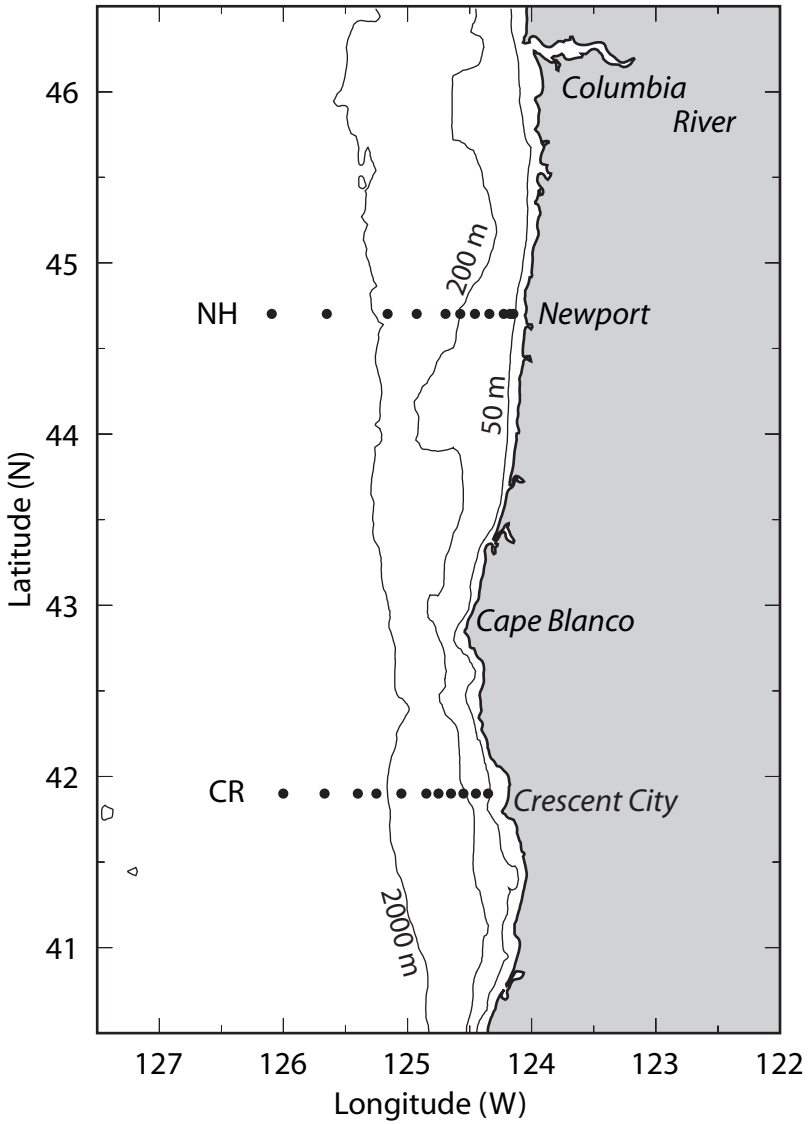

Figure 1. Shelf and coastline geometry in the region of the section pair, showing the standard CTD stations of each section, and the location of Cape Blanco, Columbia River estuary, and the 50, 200 and 2000 m isobaths.

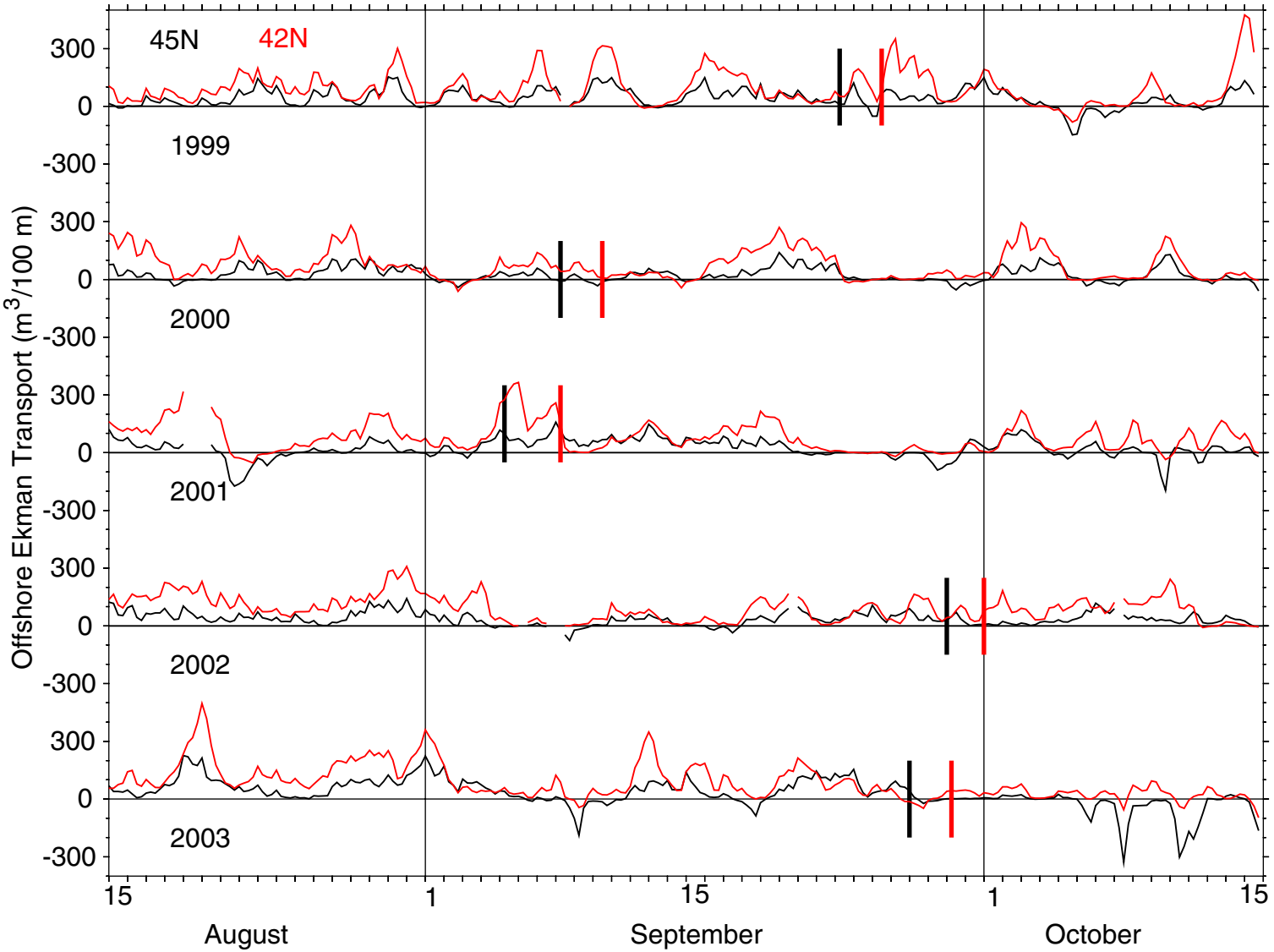

Figure 2. Six-hourly values of the coastal upwelling index at 45°N, 125°W (black) and 42°N, 125°W (red) in late summer and early autumn (15 August through 15 October) of 1999-2003. Long vertical lines indicate 1 September and 1 October. Short vertical lines indicate dates of hydrographic sampling on the NH-line (black) and the CR-line (red). (Data from http://www.pfeg.noaa.gov.)

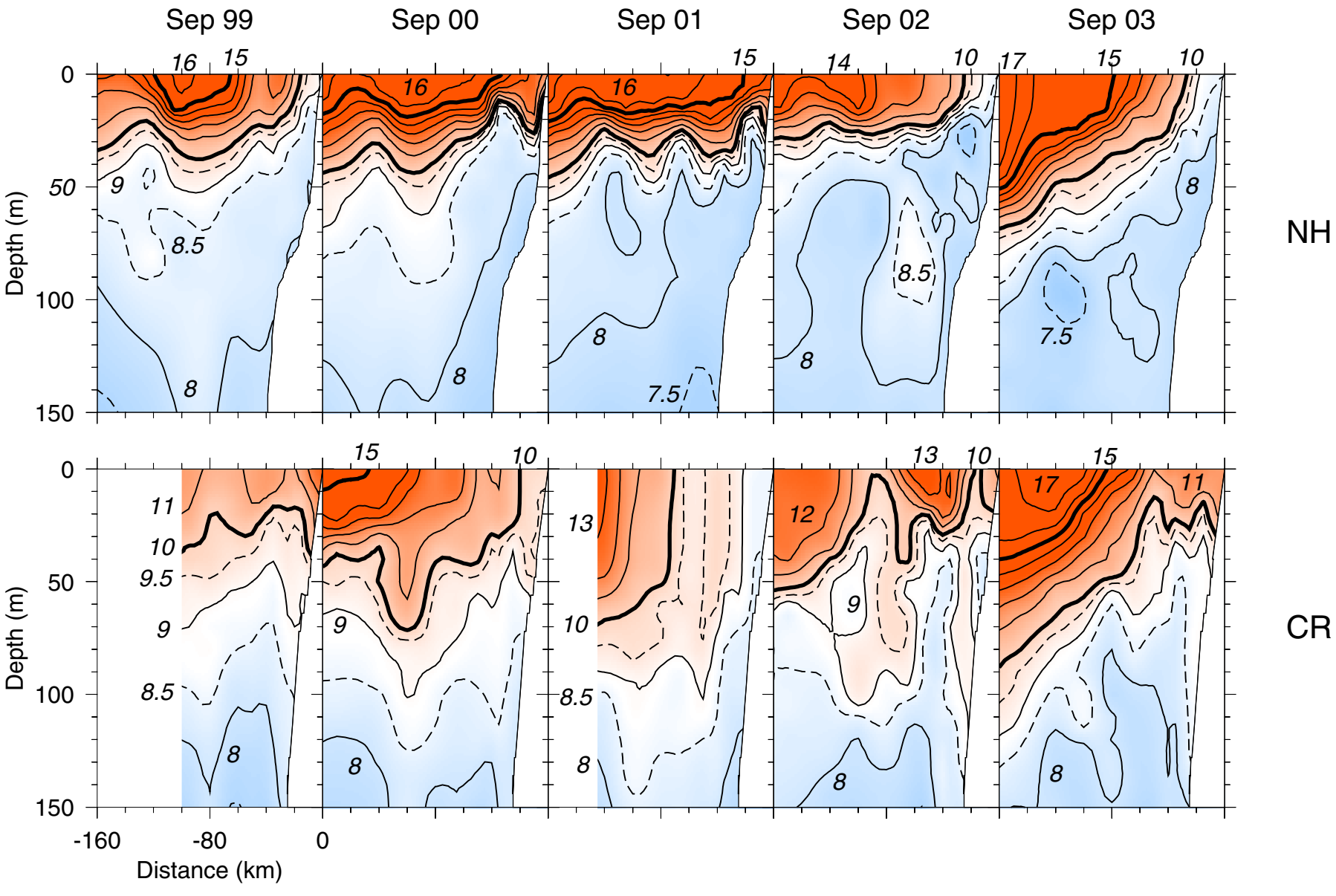

Figure 3. Upper-ocean distributions of temperature (C).

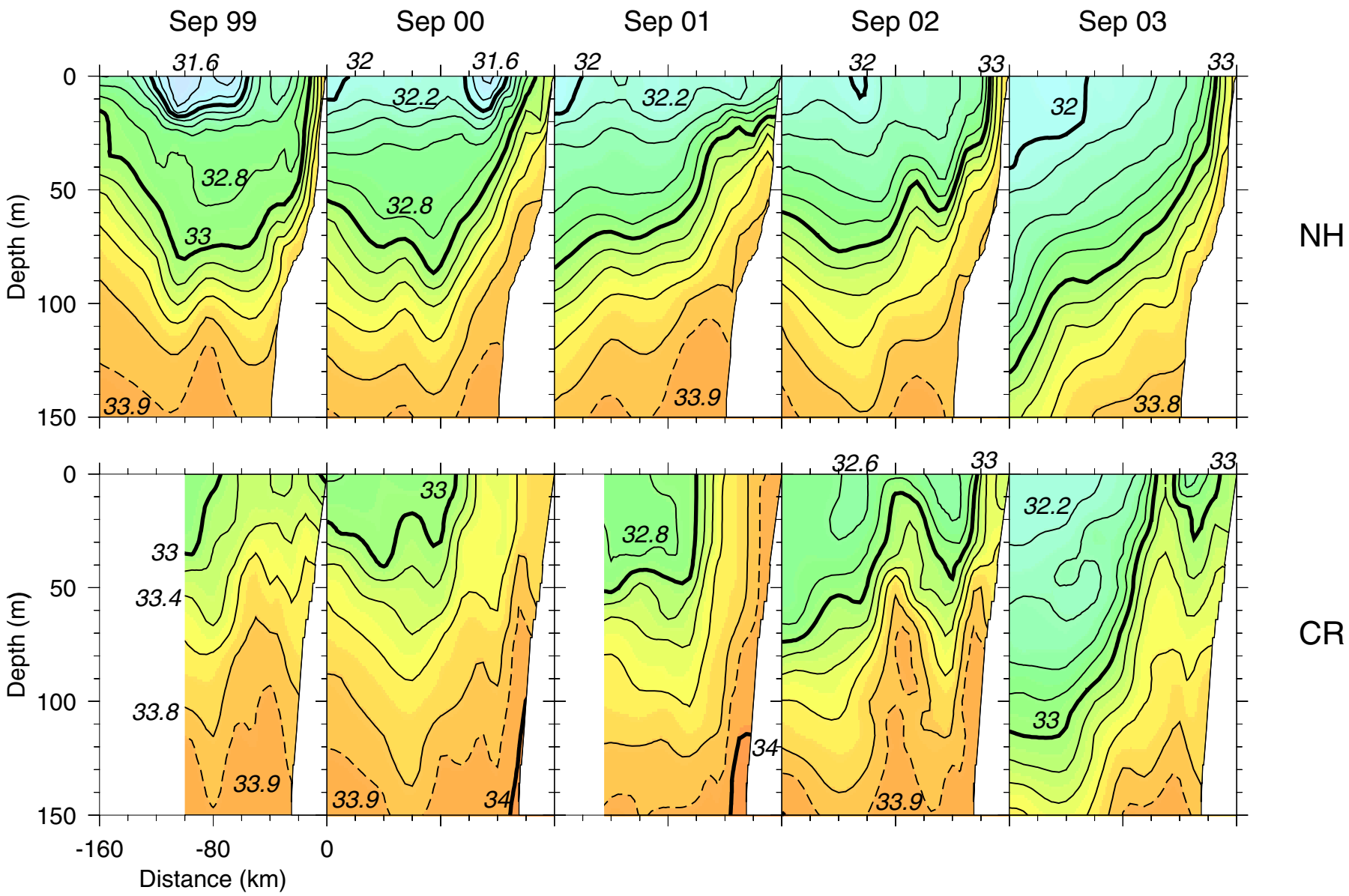

Figure 4. Upper-ocean distributions of salinity (psu).

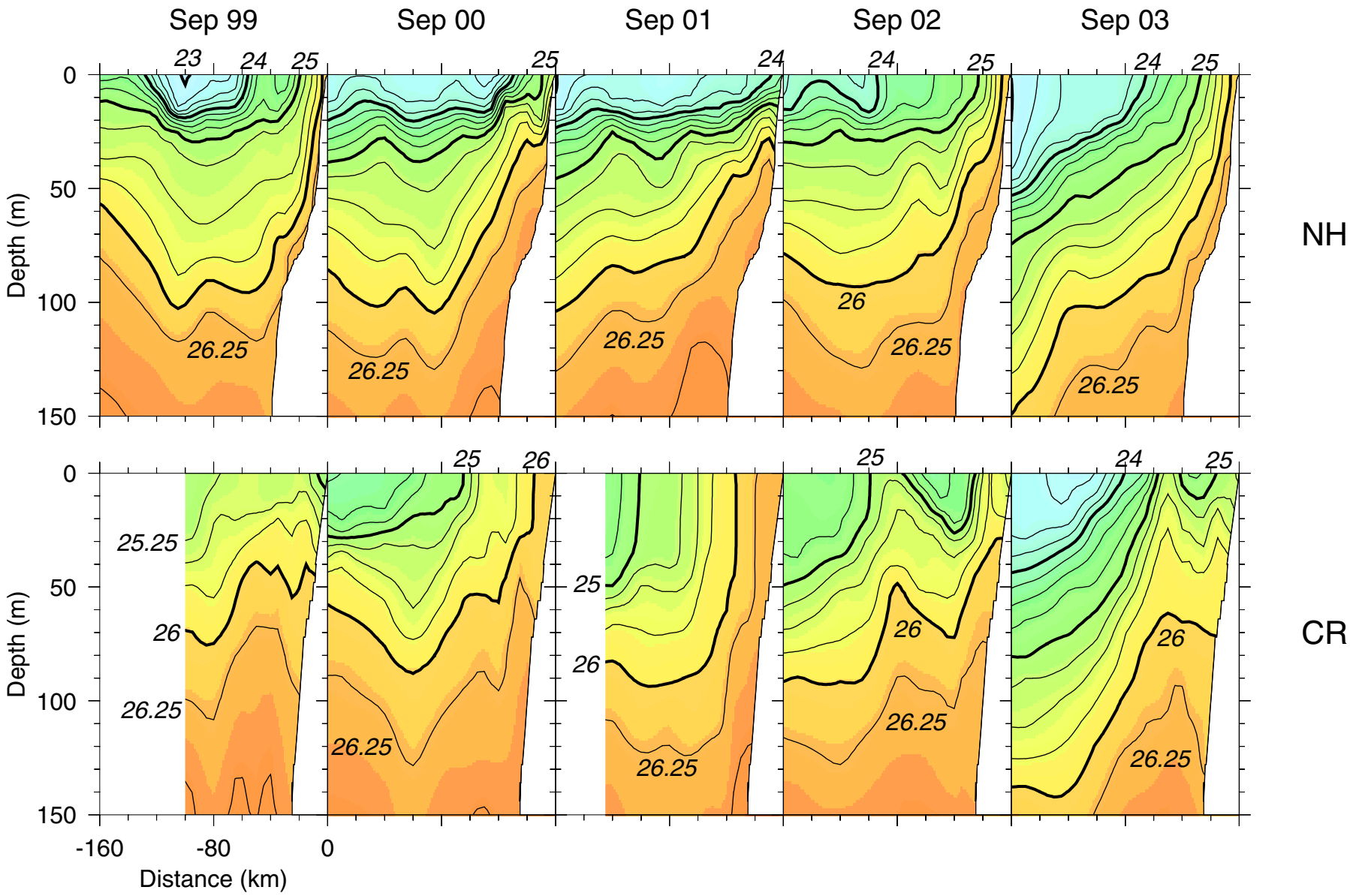

Figure 5. Upper-ocean distributions of potential density anomaly (σ_θ, kg m^{-3}).

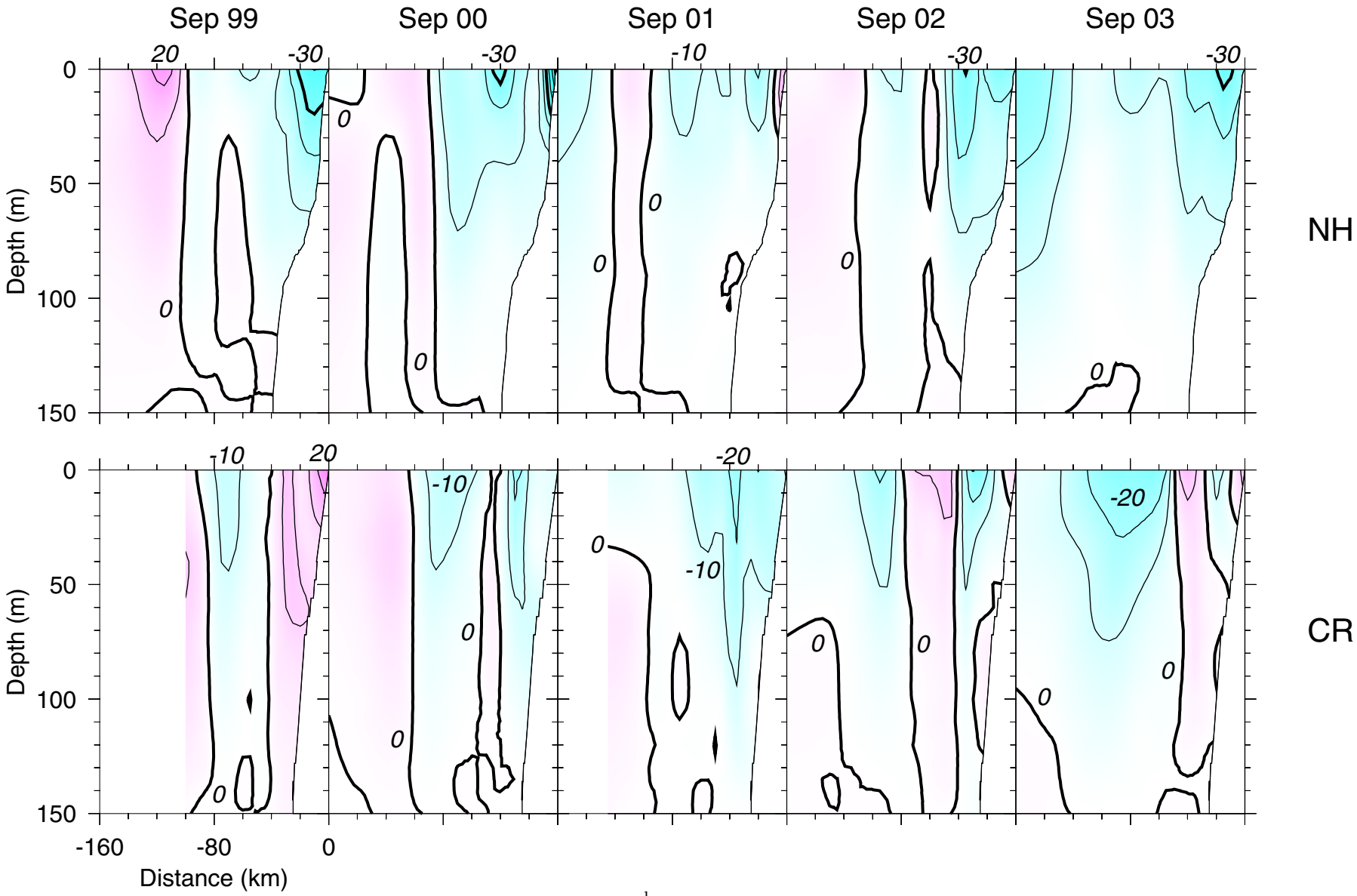

Figure 6. Upper-ocean distributions of geostrophic velocity (cm s^{-1}, positive northward) relative to 150 dbar. Values inshore of the 150 m isobath were calculated by the method of Reid and Mantyla (1976).

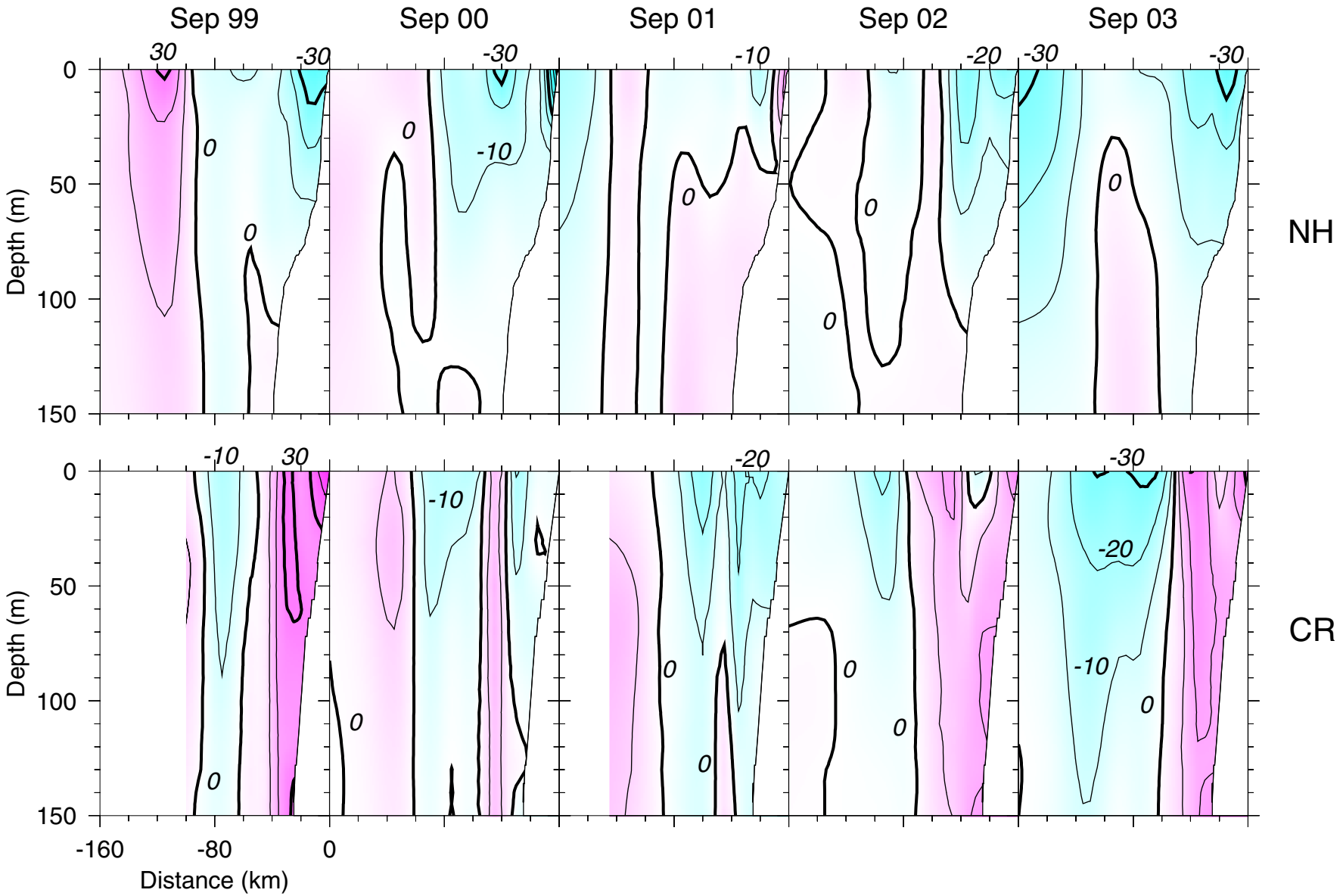

Figure 7. Upper-ocean distributions of geostrophic velocity (cm s^{-1}, positive northward) relative to 500 dbar. Values inshore of the 500 m isobath were calculated by the method of Reid and Mantyla (1976).

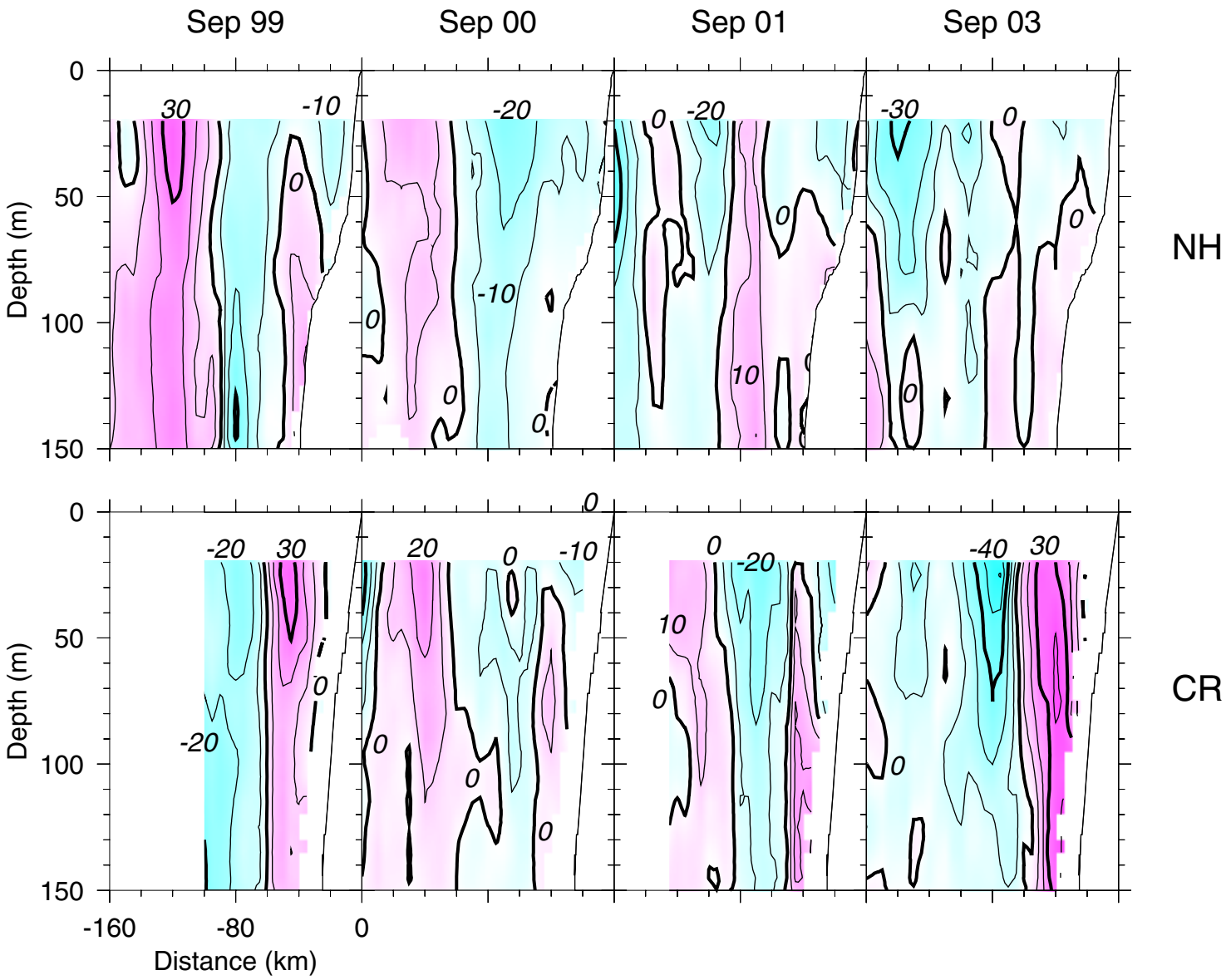

Figure 8. Upper-ocean distributions of northward (alongshore) component of ADCP velocity (cm s^{-1}).

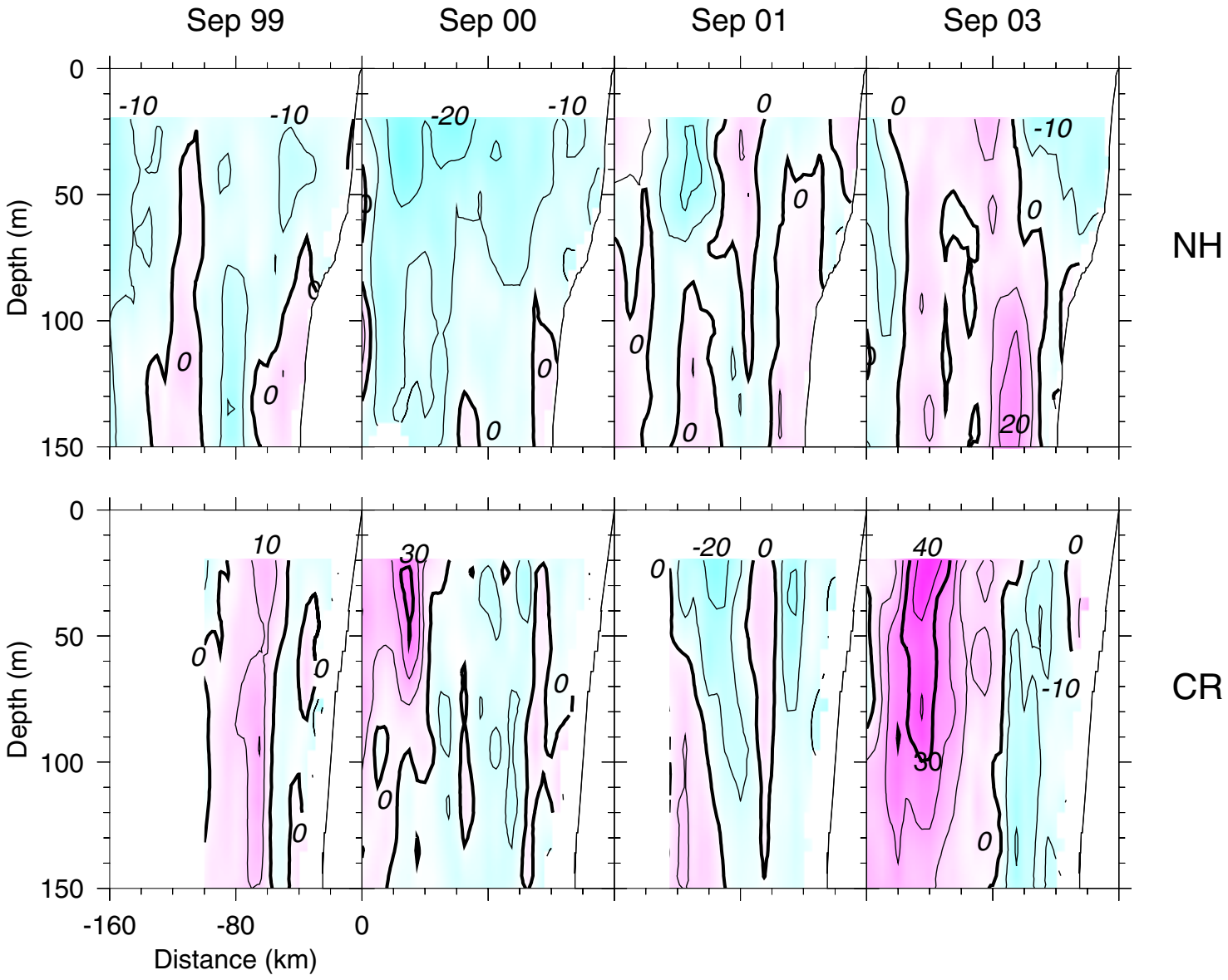

Figure 9. Upper-ocean distributions of eastward (onshore) component of ADCP velocity (cm s^{-1}).

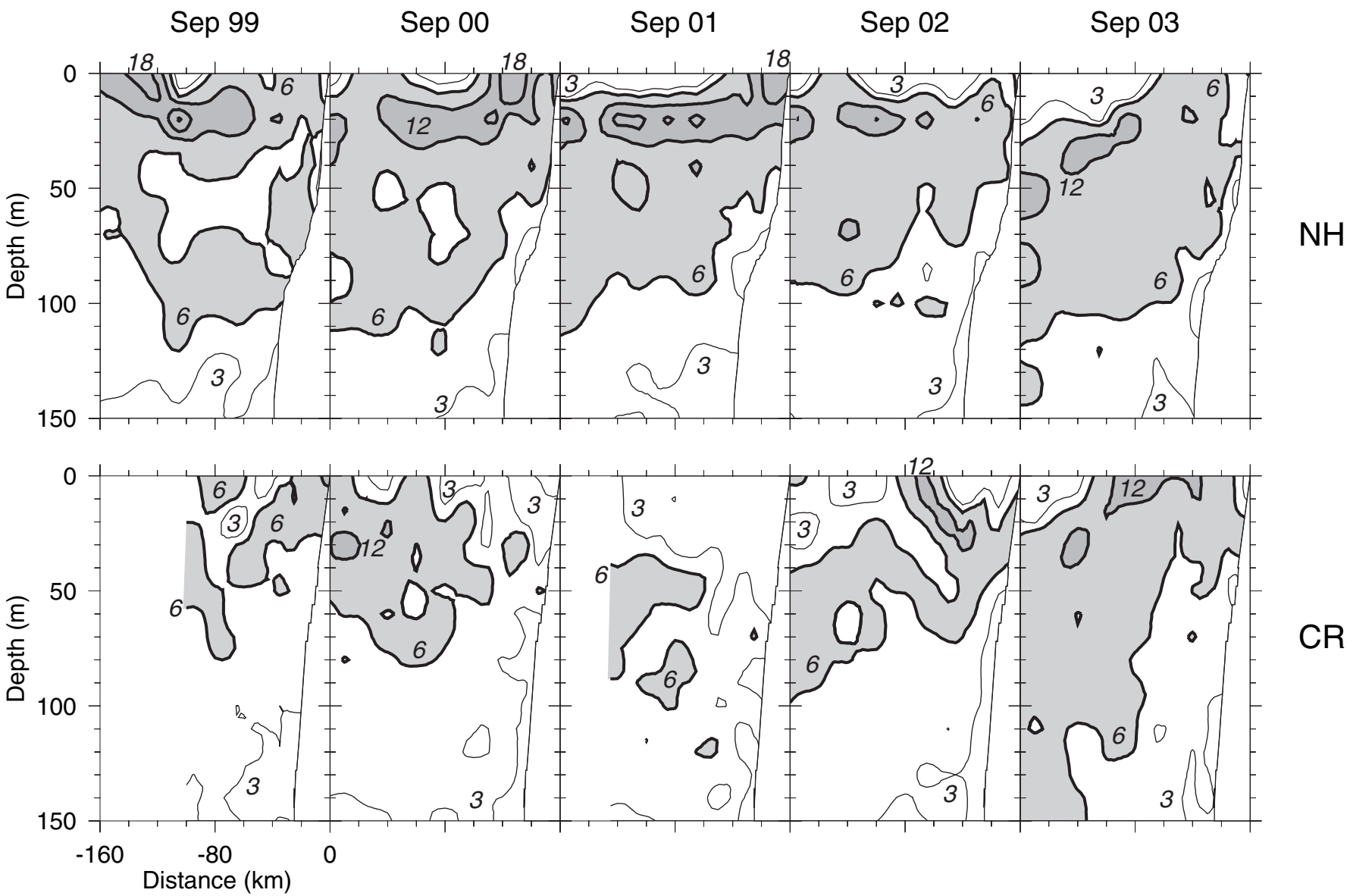

Figure 10. Upper-ocean distributions of Brunt-Vaisala frequency (cycles per hour); values were calculated at 10 m intervals as the least-squares fit over a 10-m centered bins; the shallowest value is at 9.5 m. Light contour is at 3 cph; heavy contours are at intervals of 6 cph.

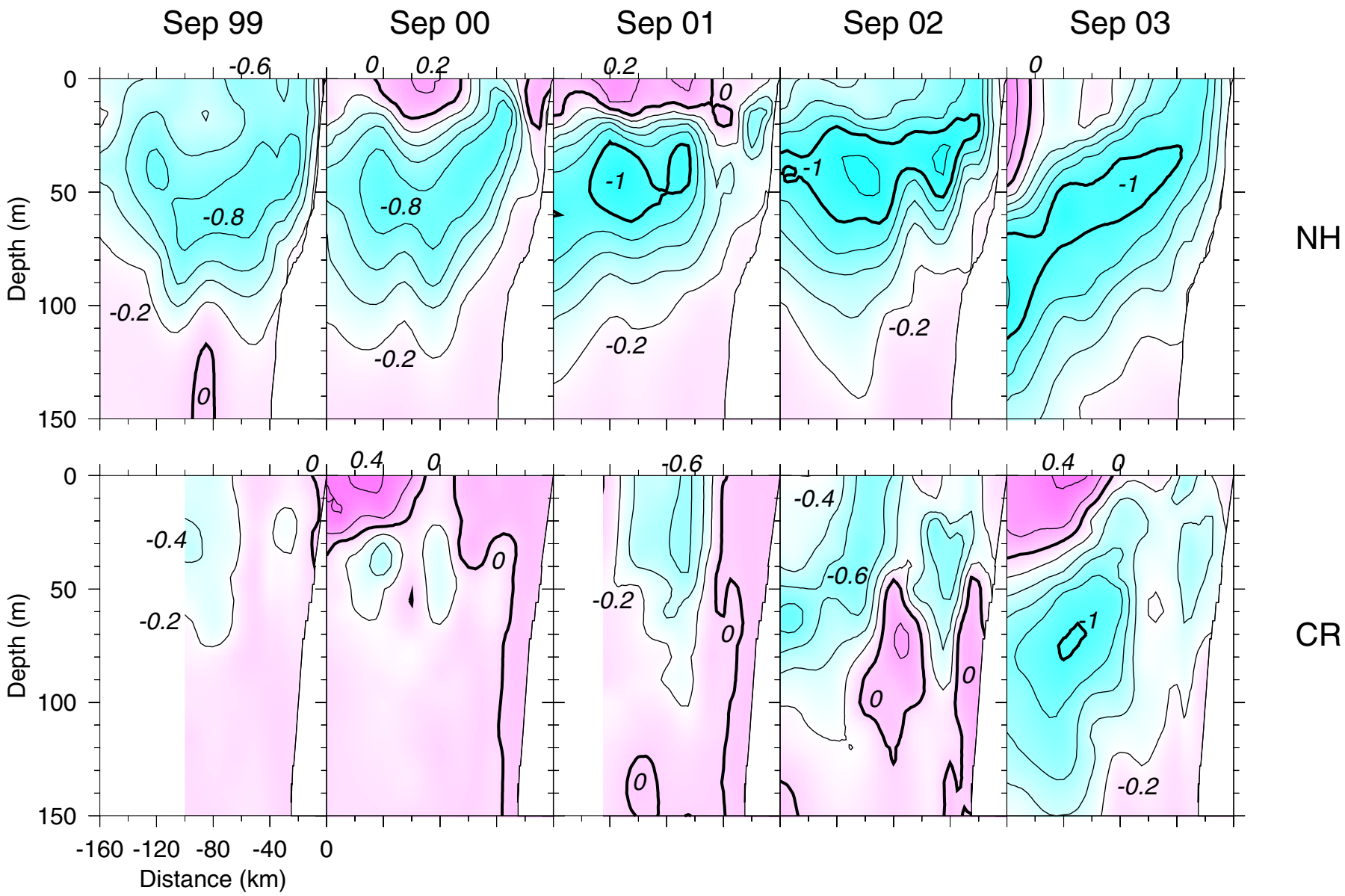

Figure 11. Upper-ocean distributions of spiciness (kg m^{-3}), calculated from T-S characteristics following Flament (2002).

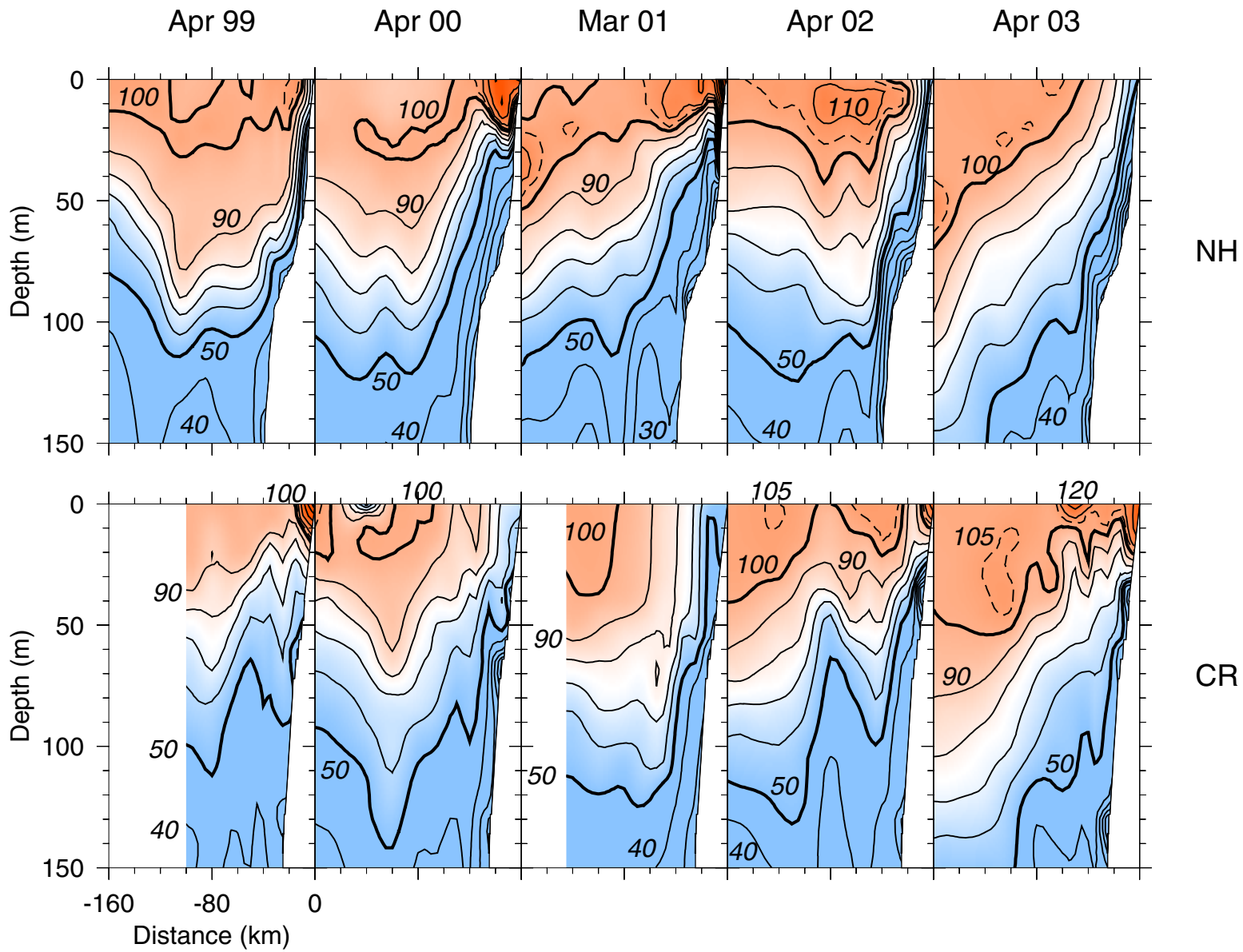

Figure 12. Upper-ocean distributions of oxygen saturation (%). Contour interval is 10 %; the 50 % and 100% contours are heavy and the 105% contour is dashed. Saturation percentage was calculated from CTD oxygen concentration data calibrated by Winkler-titrated samples from a few stations on each cruise, using the algorithm from the Scripps PACODF library.

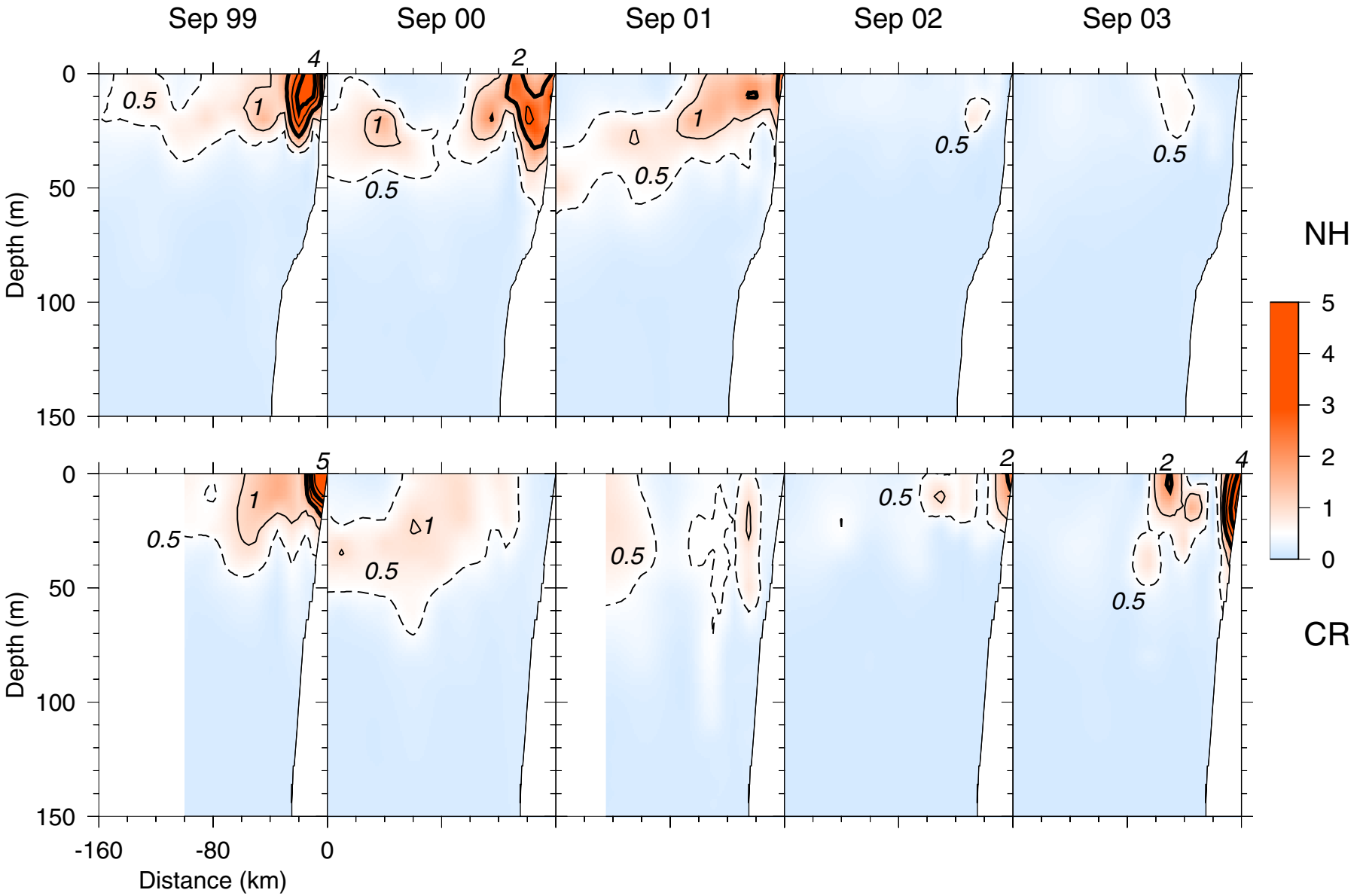

Figure 13. Upper-ocean distributions of fluorescence voltage (V). Contours: dashed at 0.5 V; thin at 1, 3; heavy at 2, 4; full scale is at 15 V in 2002 and at 5.0 V in other years. Fluorometer calibration is believed to remain about the same within each cruise though it may vary from cruise to cruise.

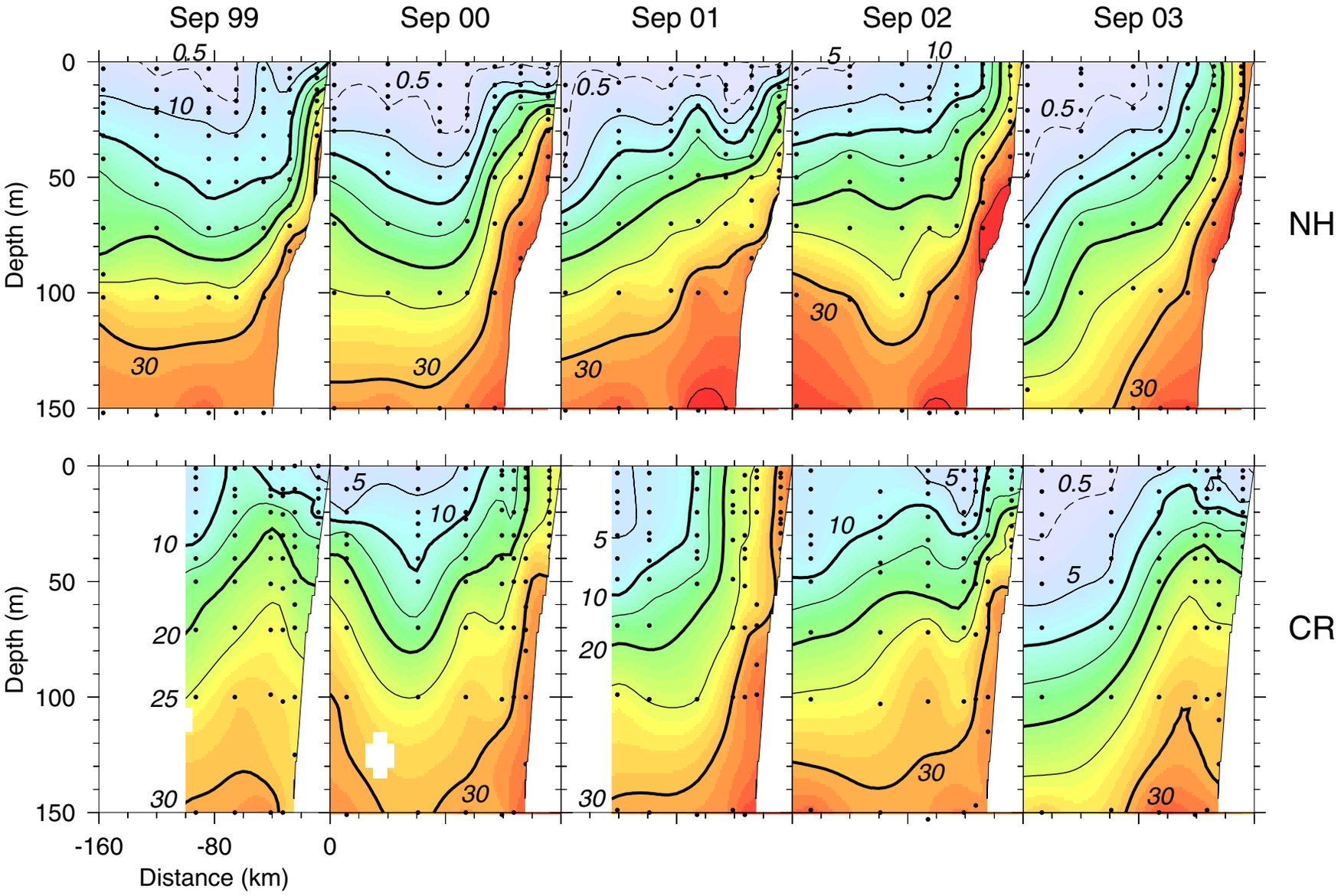

Figure 14. Upper-ocean distributions of total nitrate (μmol/l).

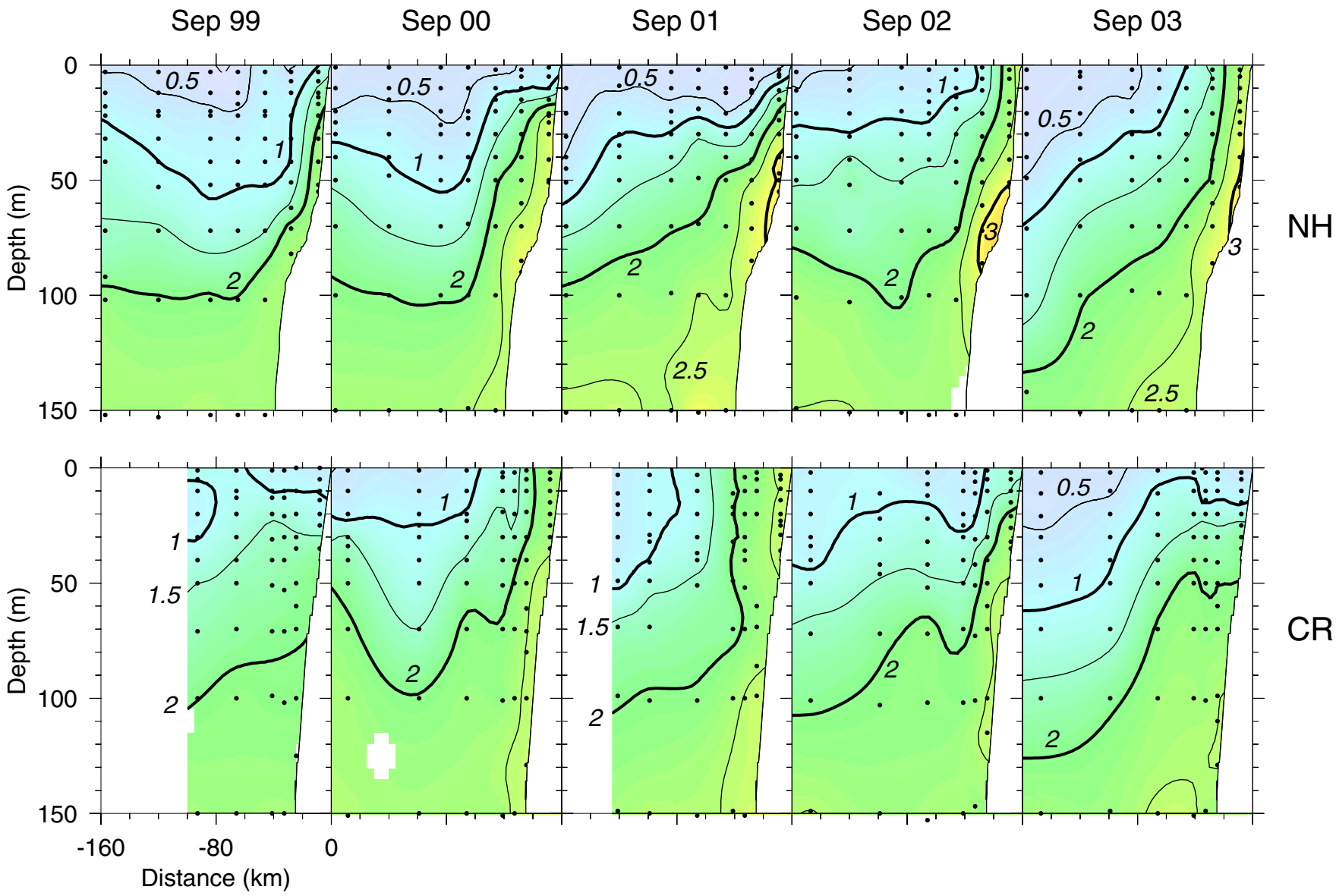

Figure 15. Upper-ocean distributions of phosphate (μmol/l).

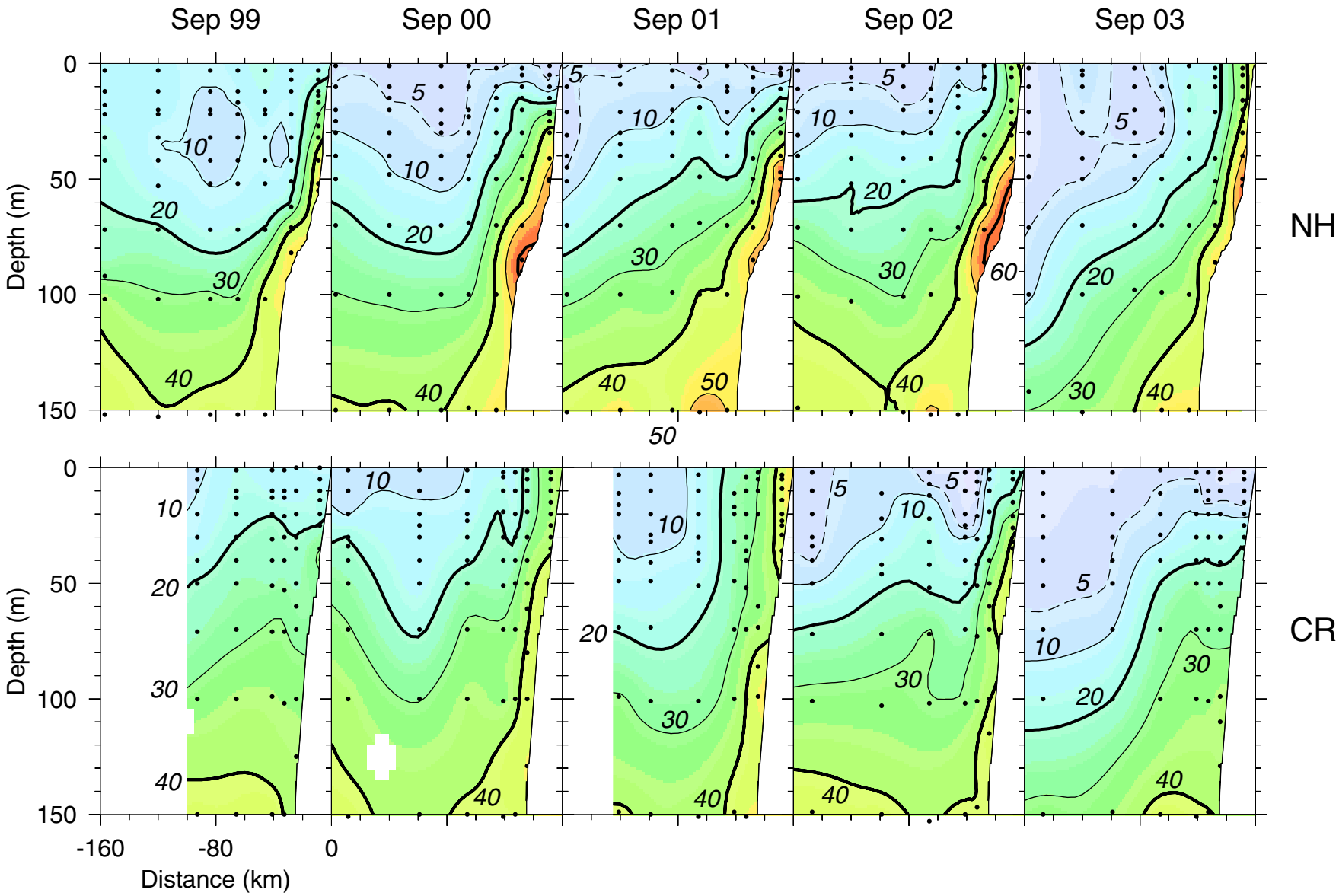

Figure 16. Upper-ocean distributions of silicate (µmol/l).

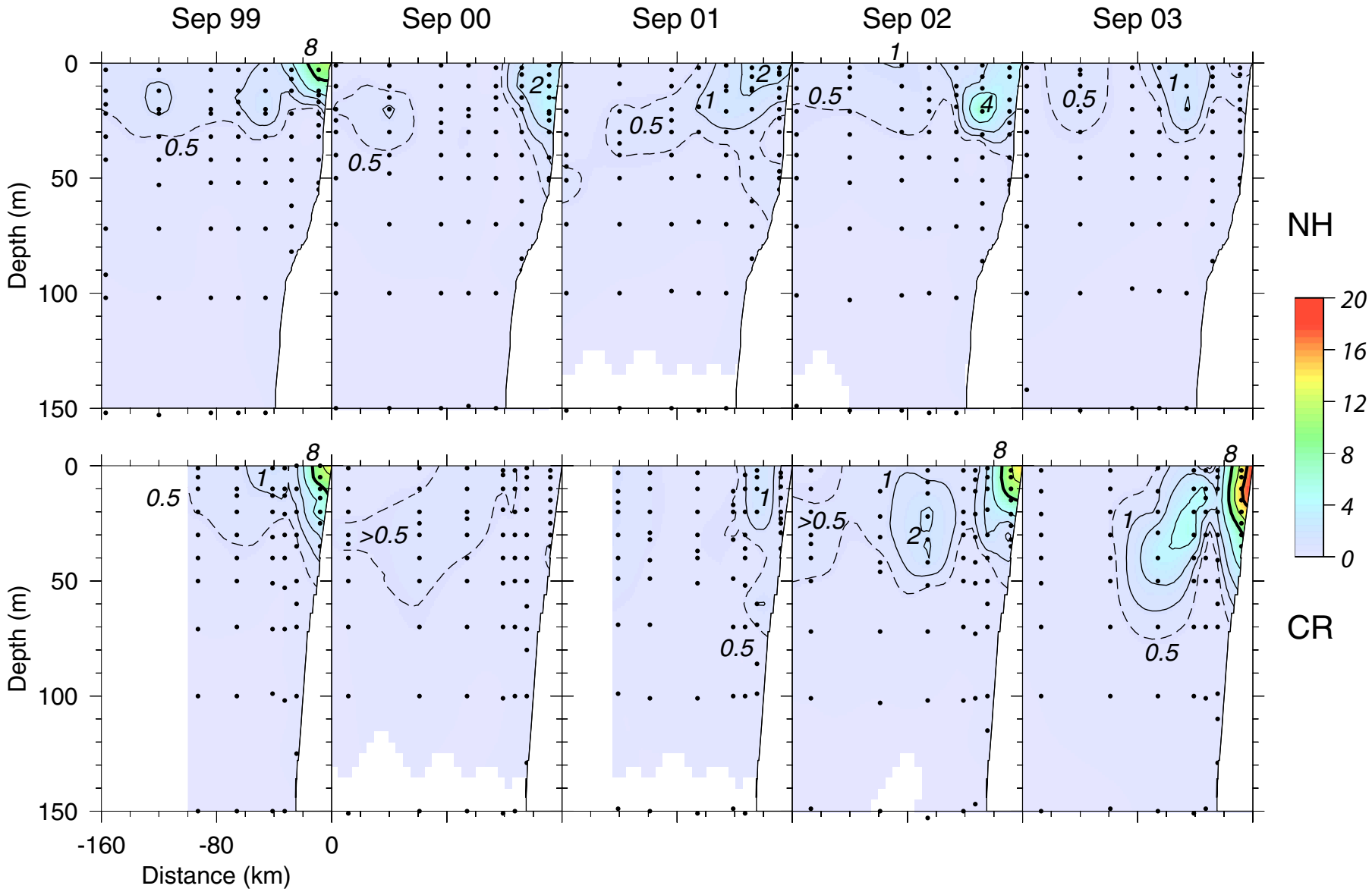

Figure 17. Upper-ocean distributions of chlorophyll (mg/m^3). Contours are at 0.5 (dashed), 1, and 2, 4, 8 (heavy), 12 and 16 mg/m^3.

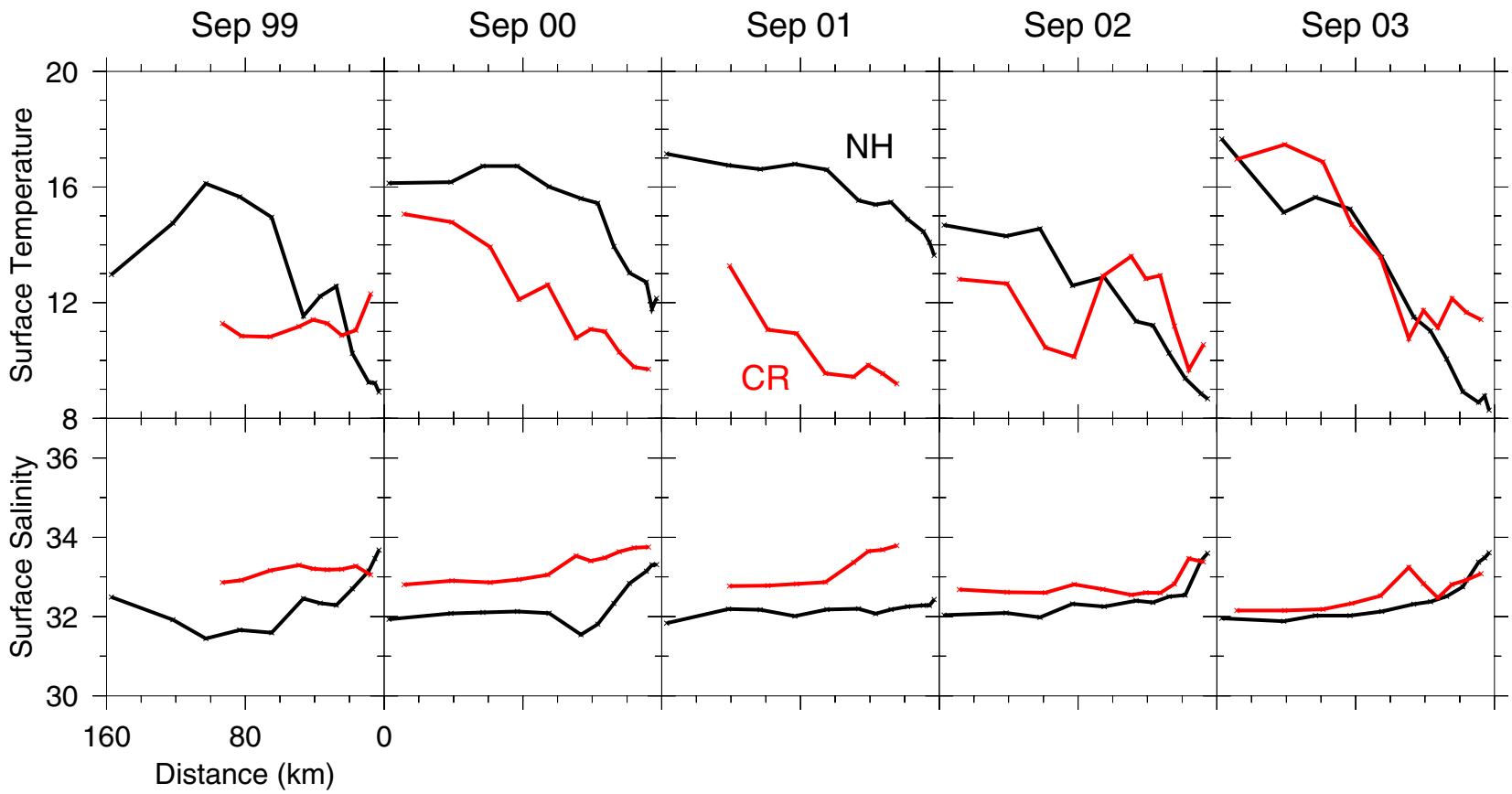

Figure 18. Offshore profiles of surface temperature and salinity.

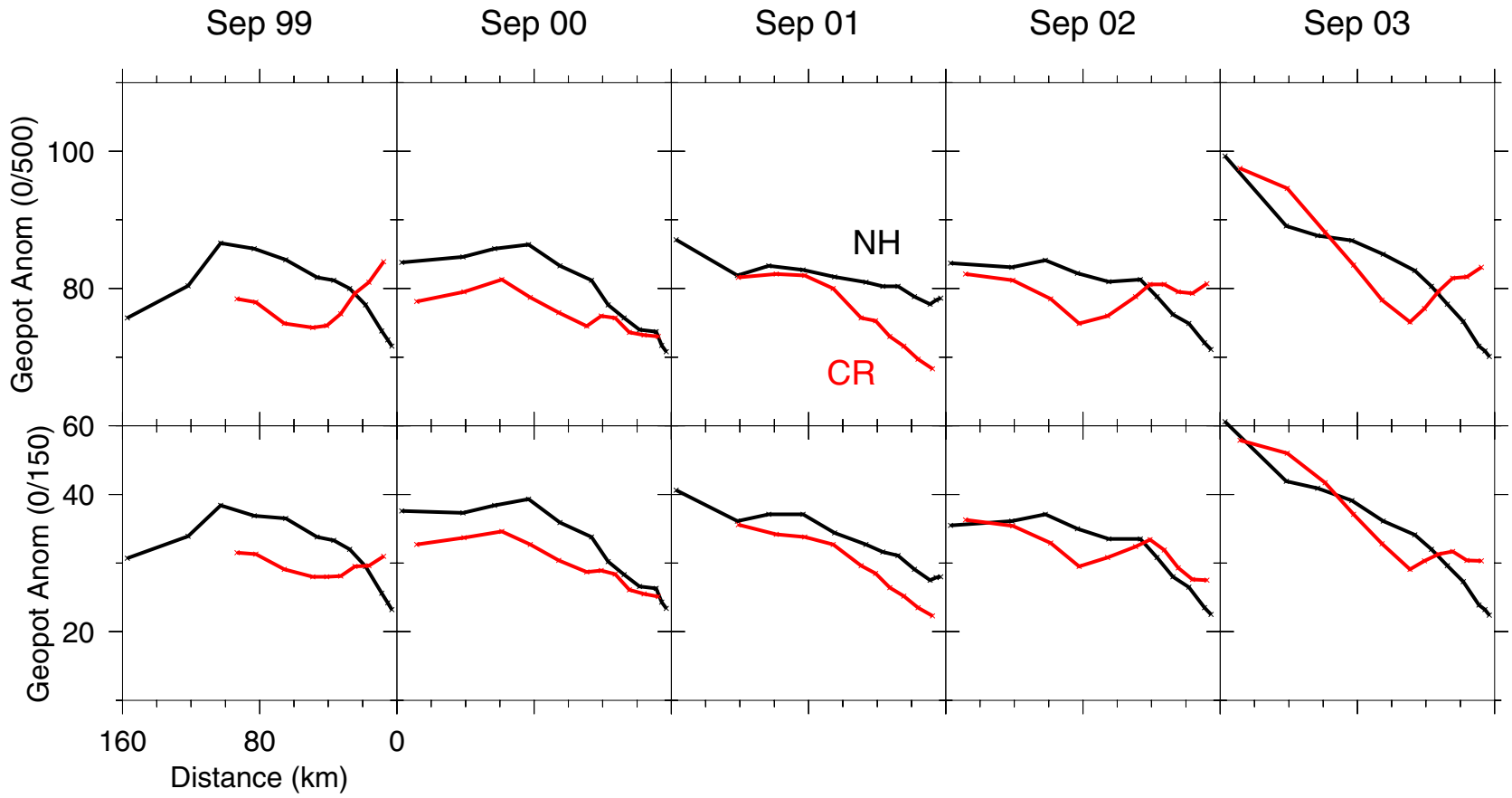

Figure 19. Offshore profiles of steric height (J/kg) of the sea surface relative to 150 dbar and 500 dbar.

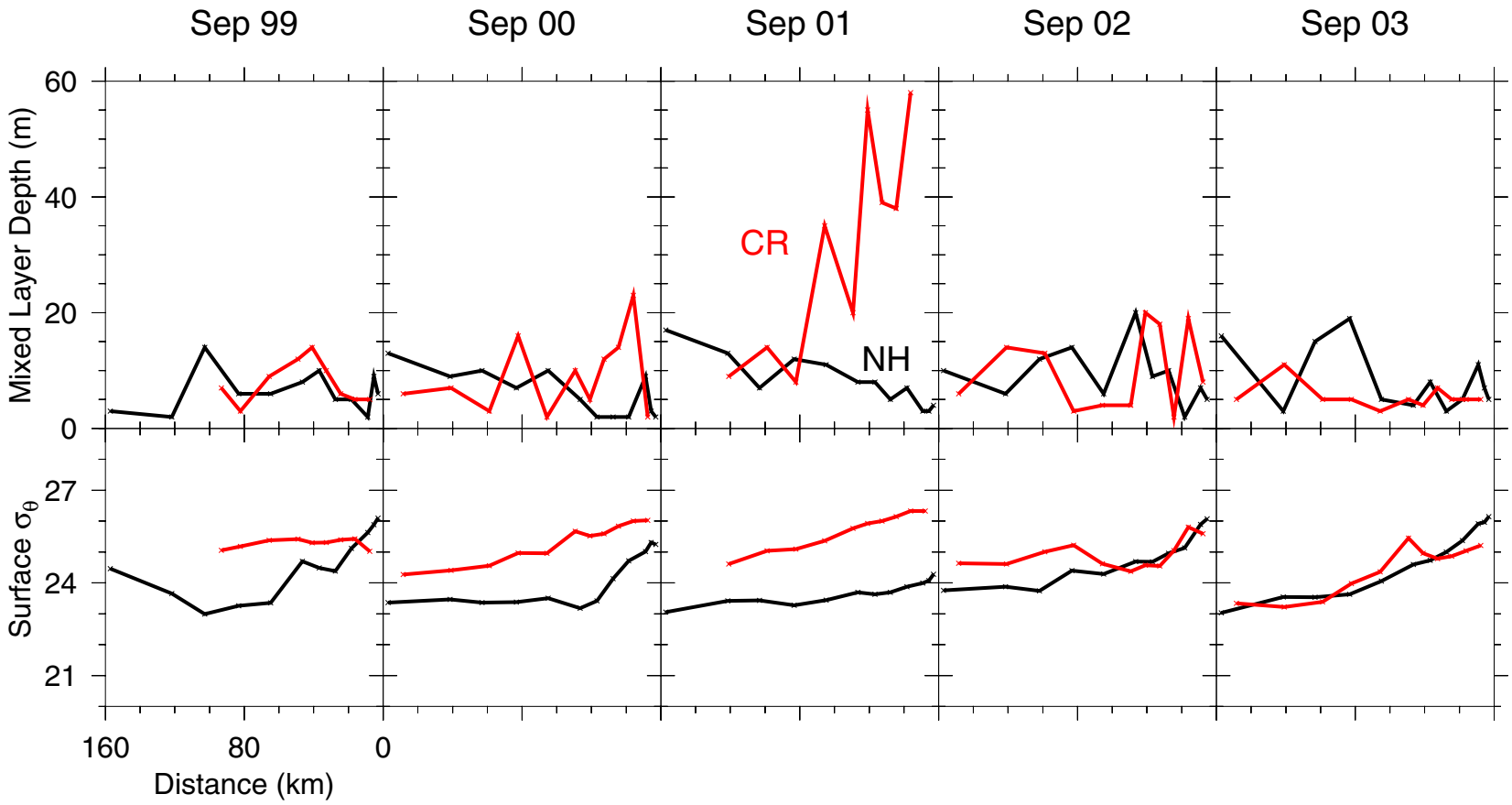

Figure 20. Offshore profiles of surface density and of surface mixed layer depth, defined as the depth at which potential density exceeds the surface value by 0.01 kg m^{-3}.

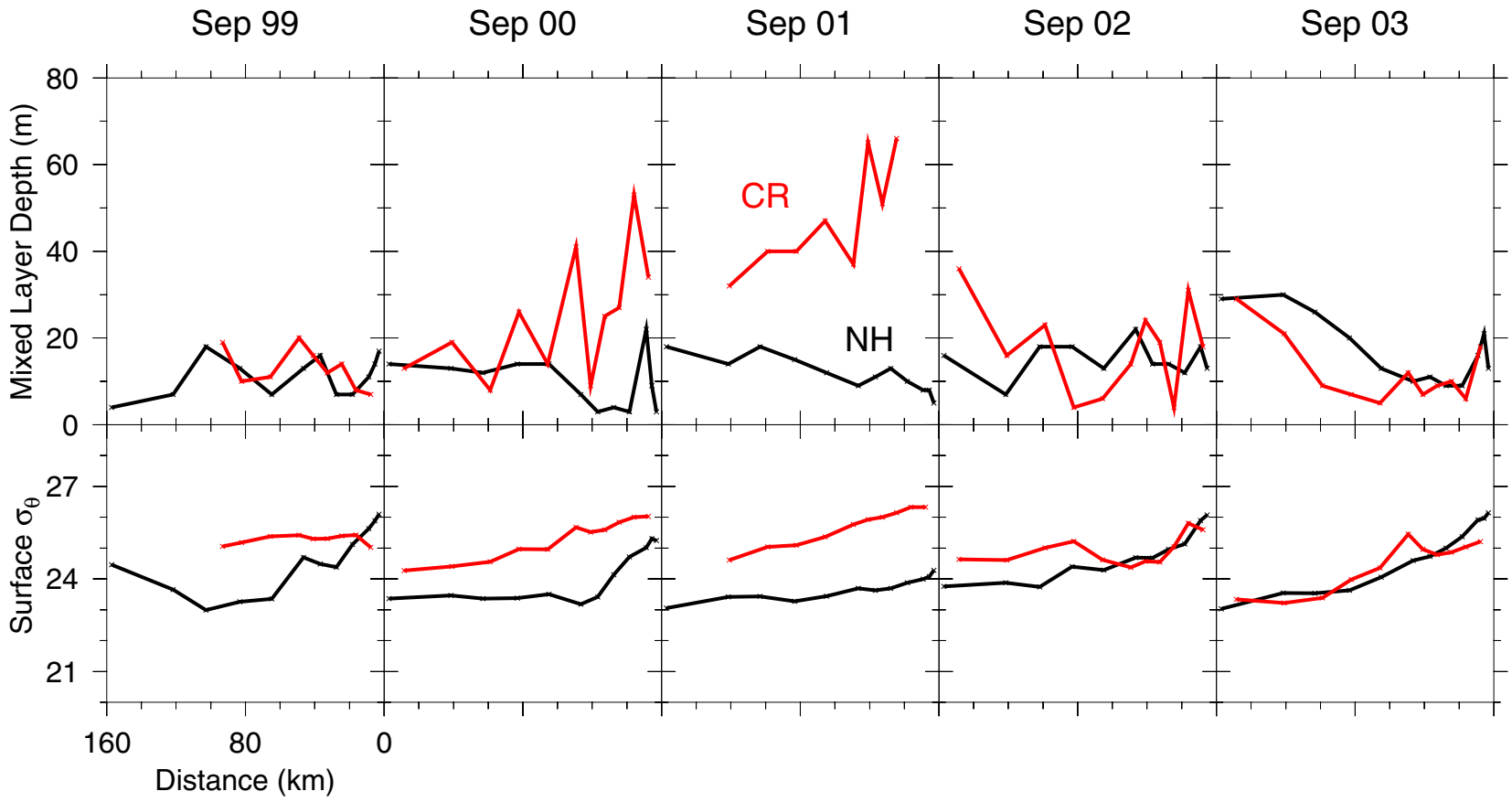

Figure 21. Offshore profiles of surface density and of surface mixed layer depth, defined as the depth at which potential density exceeds the surface value by 0.1 kg m^{-3}.

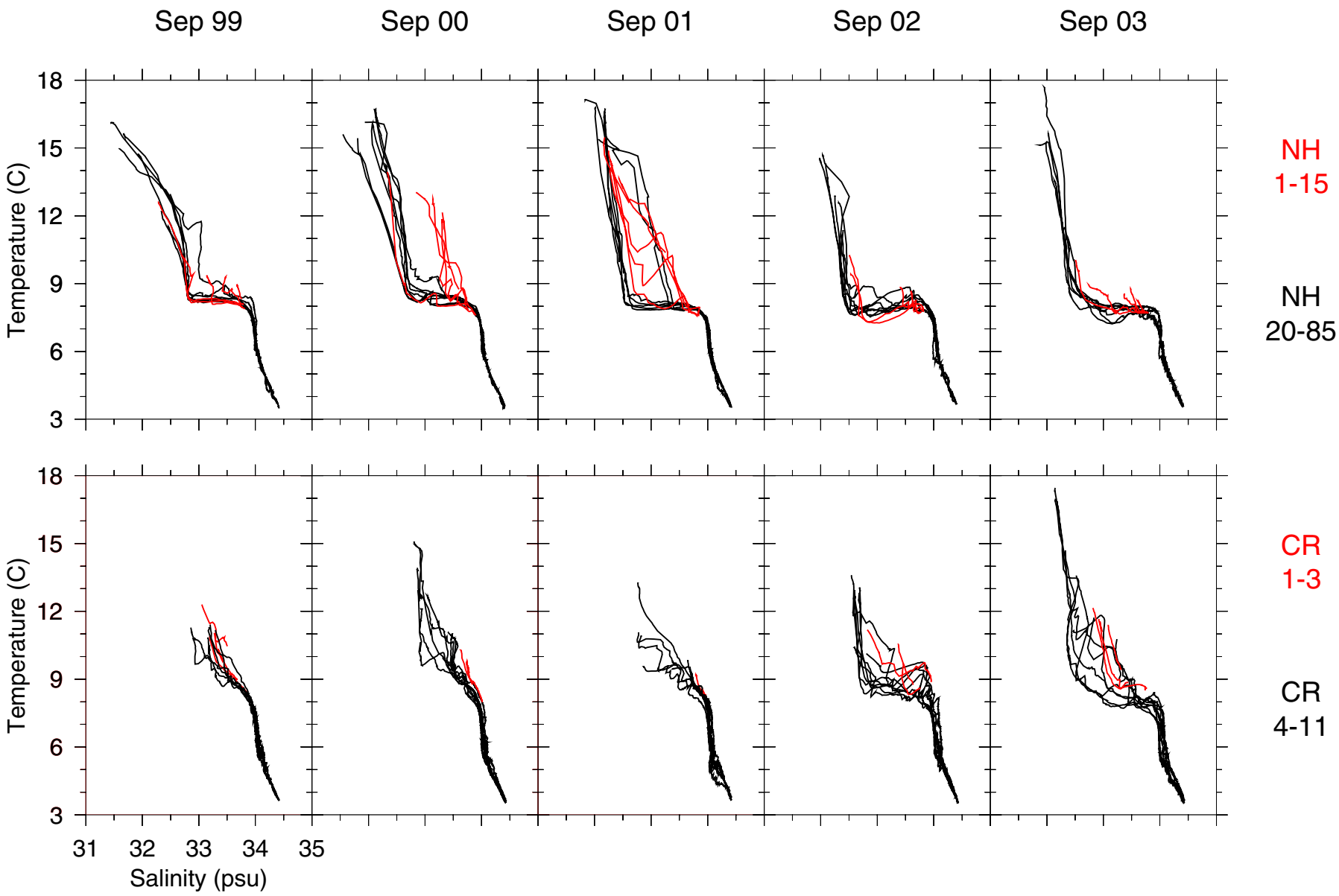

Figure 22. T-S characteristics of all CTD stations. Shelf stations are plotted in red.

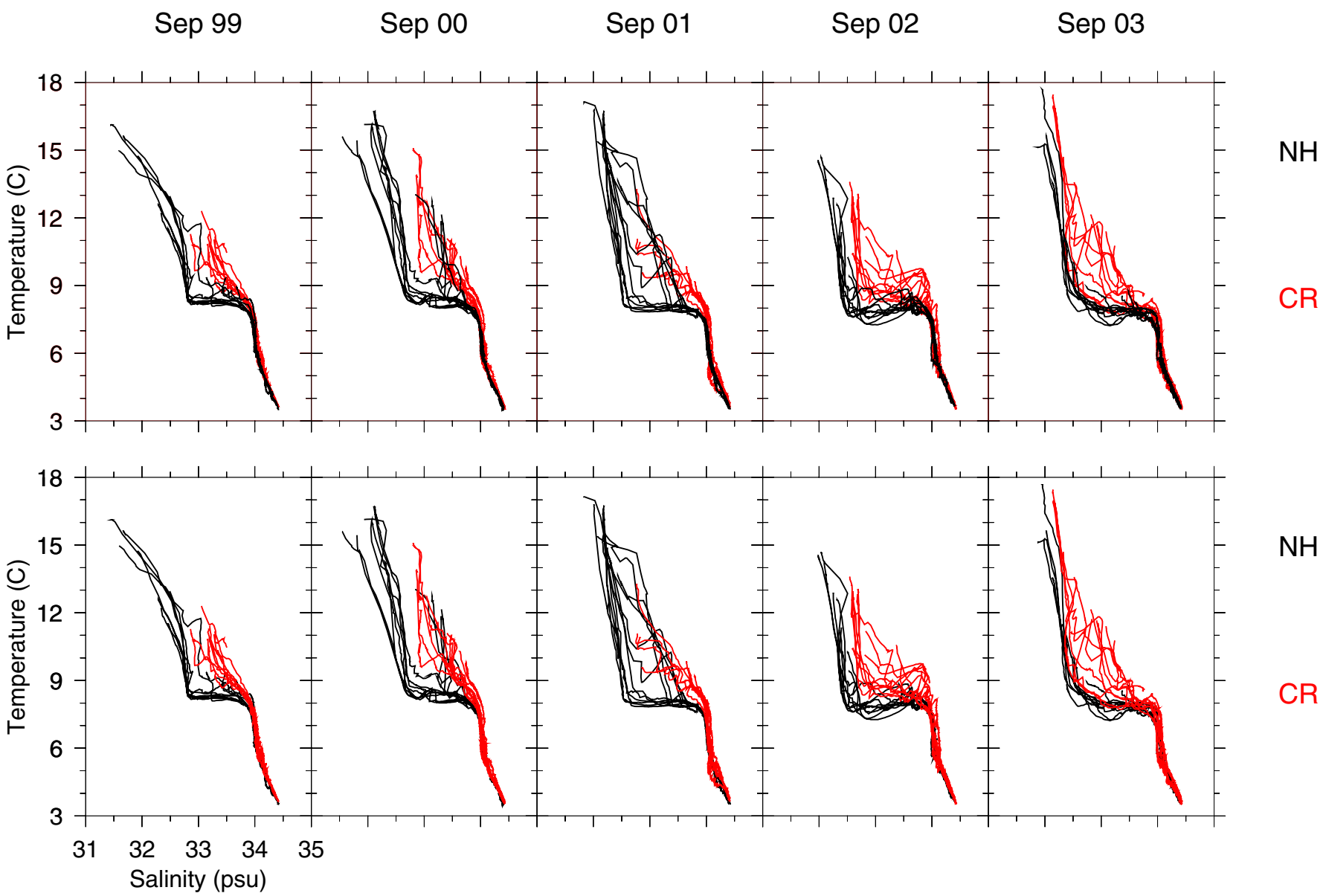

Figure 23. Superimposed groups of T-S characteristics. Upper row: NH (black) on CR (red). Lower row: CR (red) on NH (black).

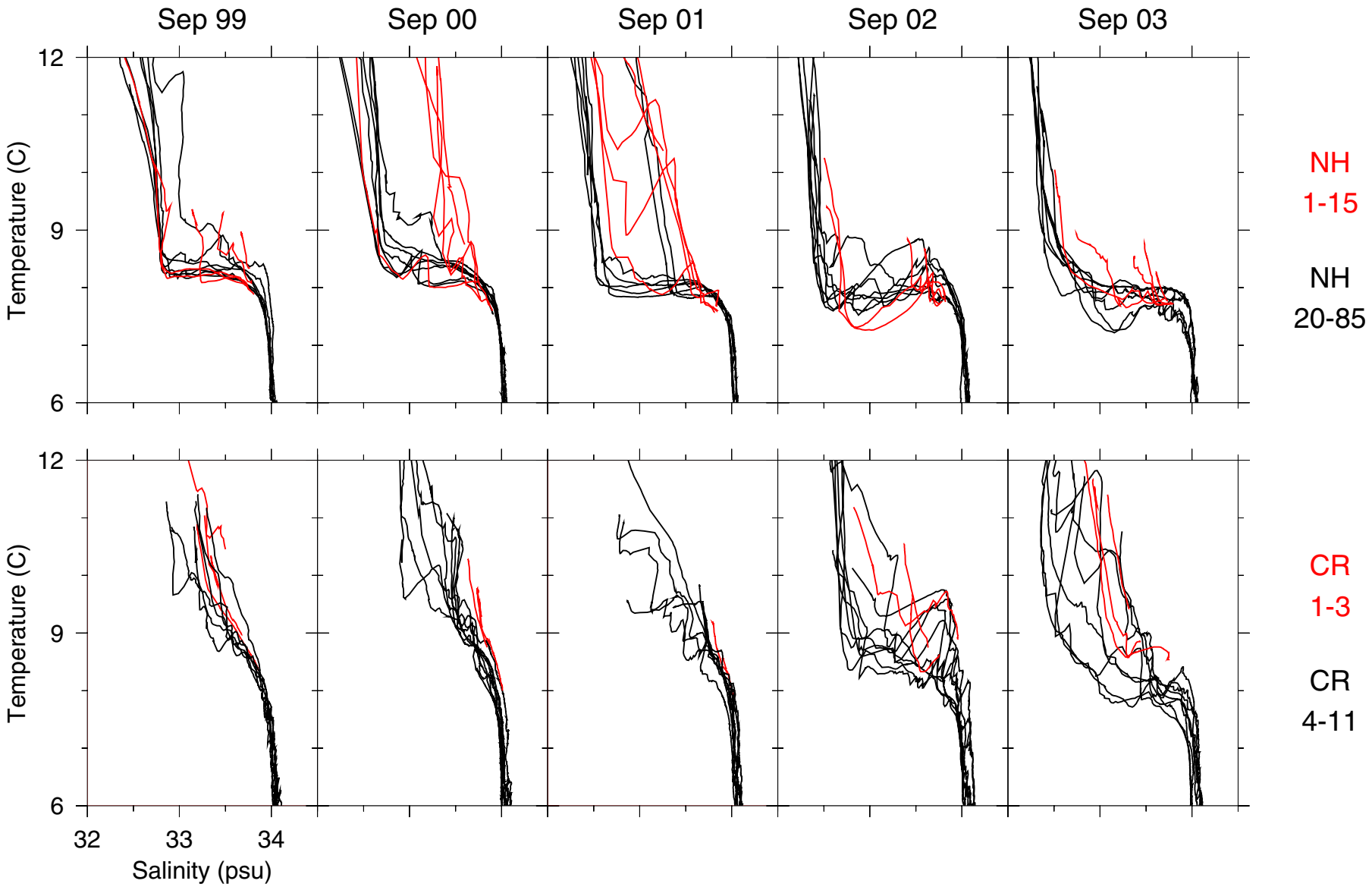

Figure 24. Detail of T-S characteristics in the permanent halocline. Shelf stations are plotted in red.

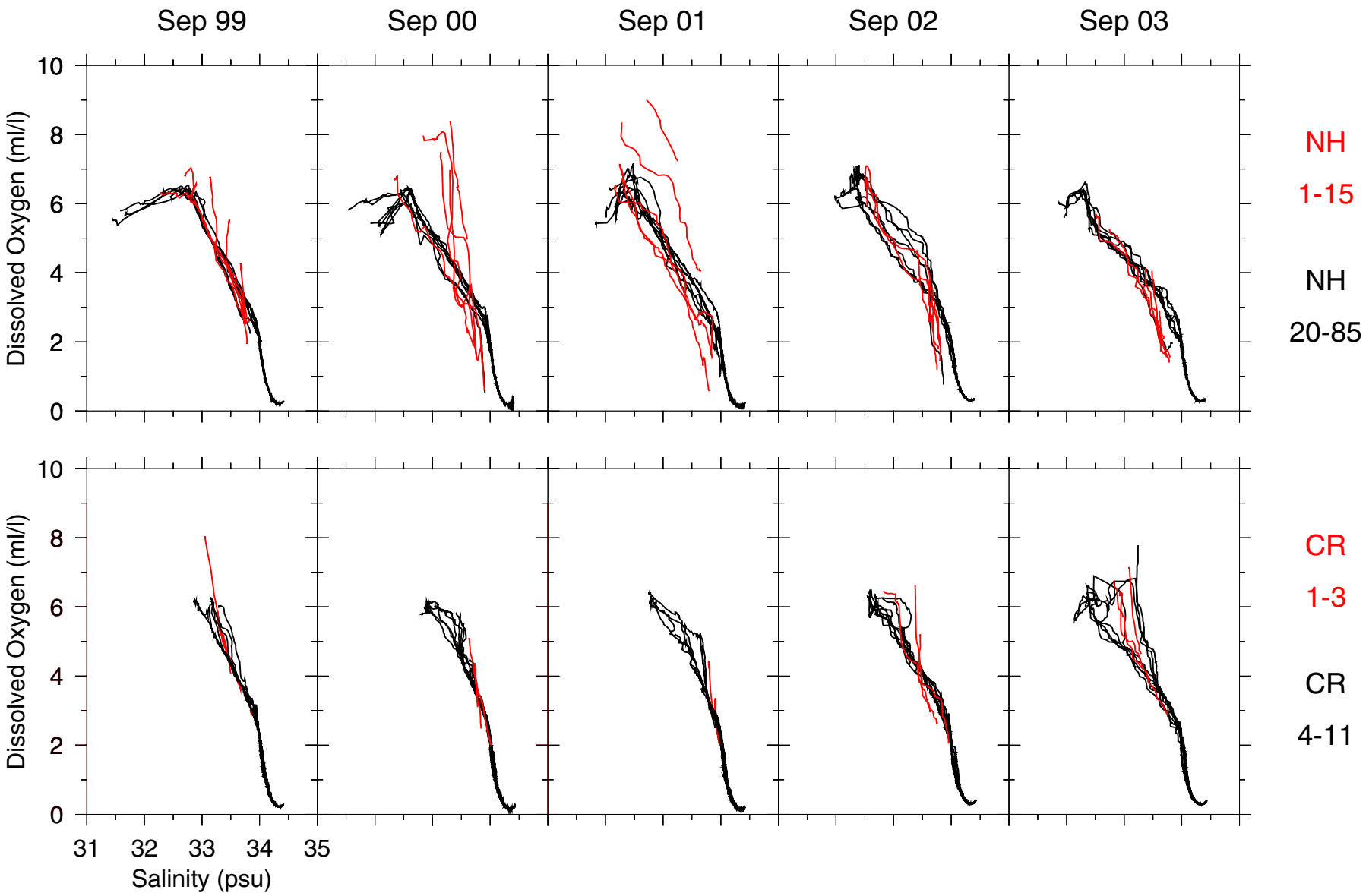

Figure 25. Oxygen-salinity characteristics of all CTD stations. Shelf stations are plotted in red.

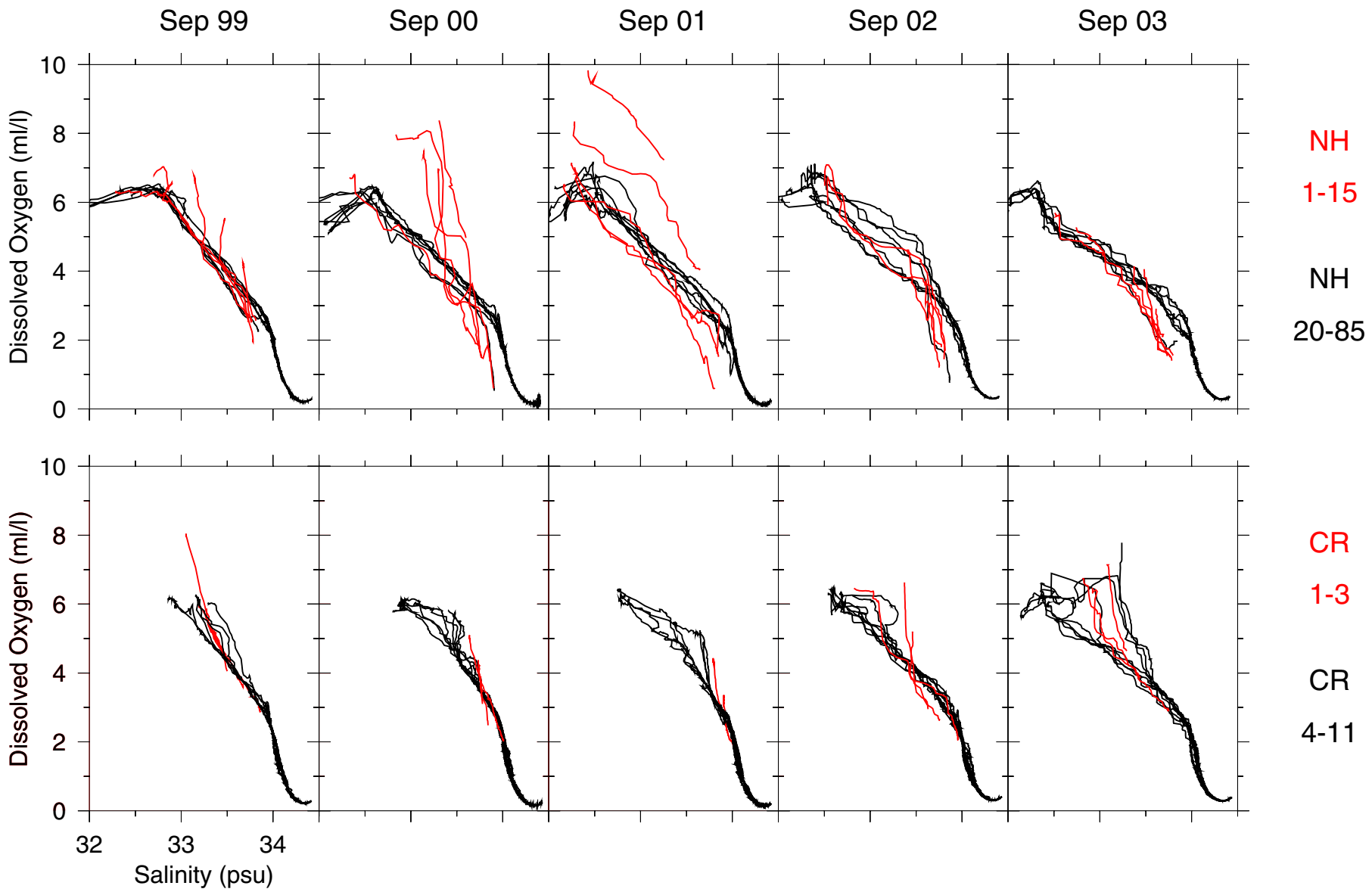

Figure 26. Detail of oxygen-salinity characteristics in and below the permanent halocline. Shelf stations are plotted in red.

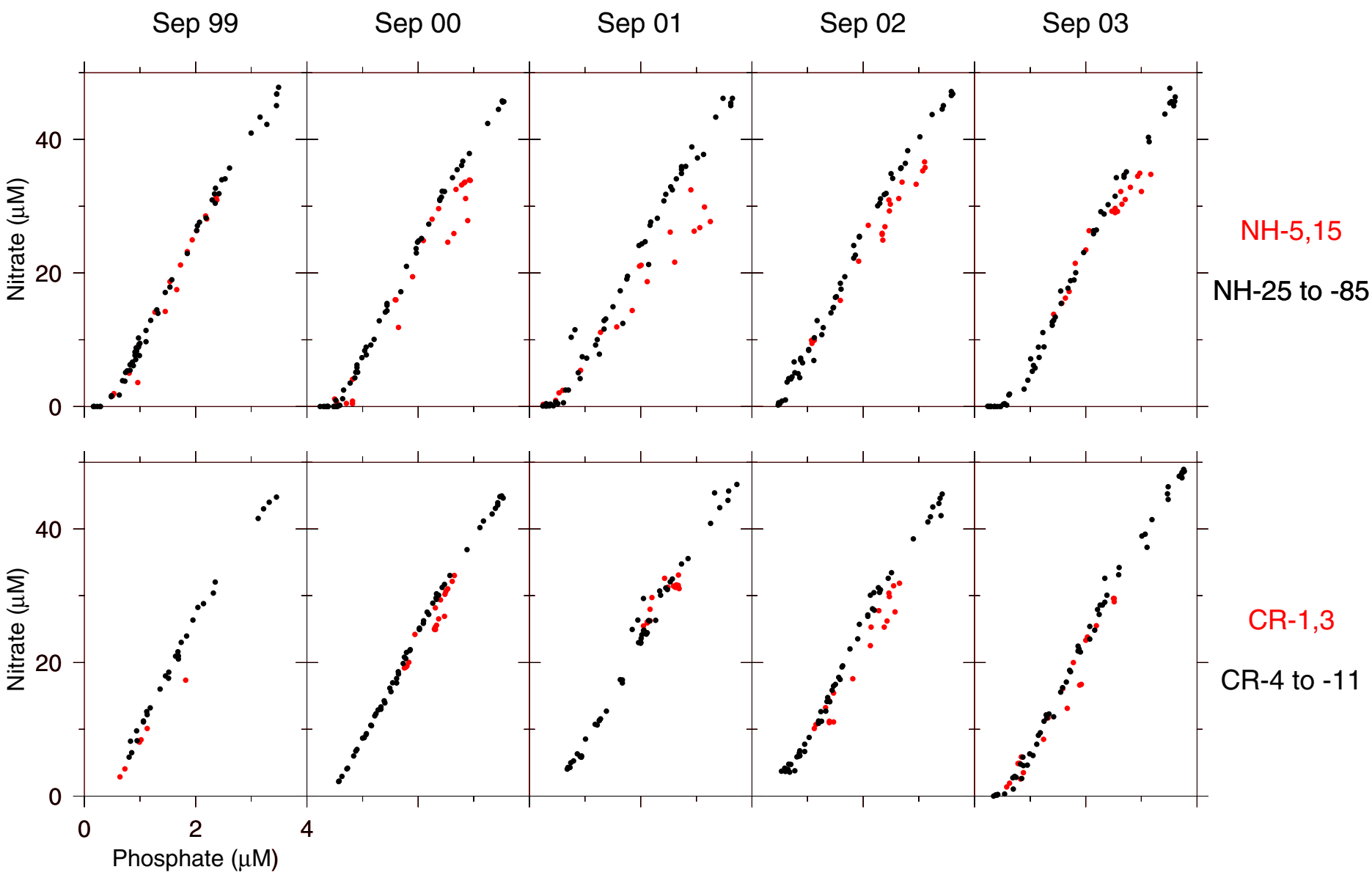

Figure 27. Nitrate-phosphate relations for all rosette samples. Shelf stations are plotted in red.

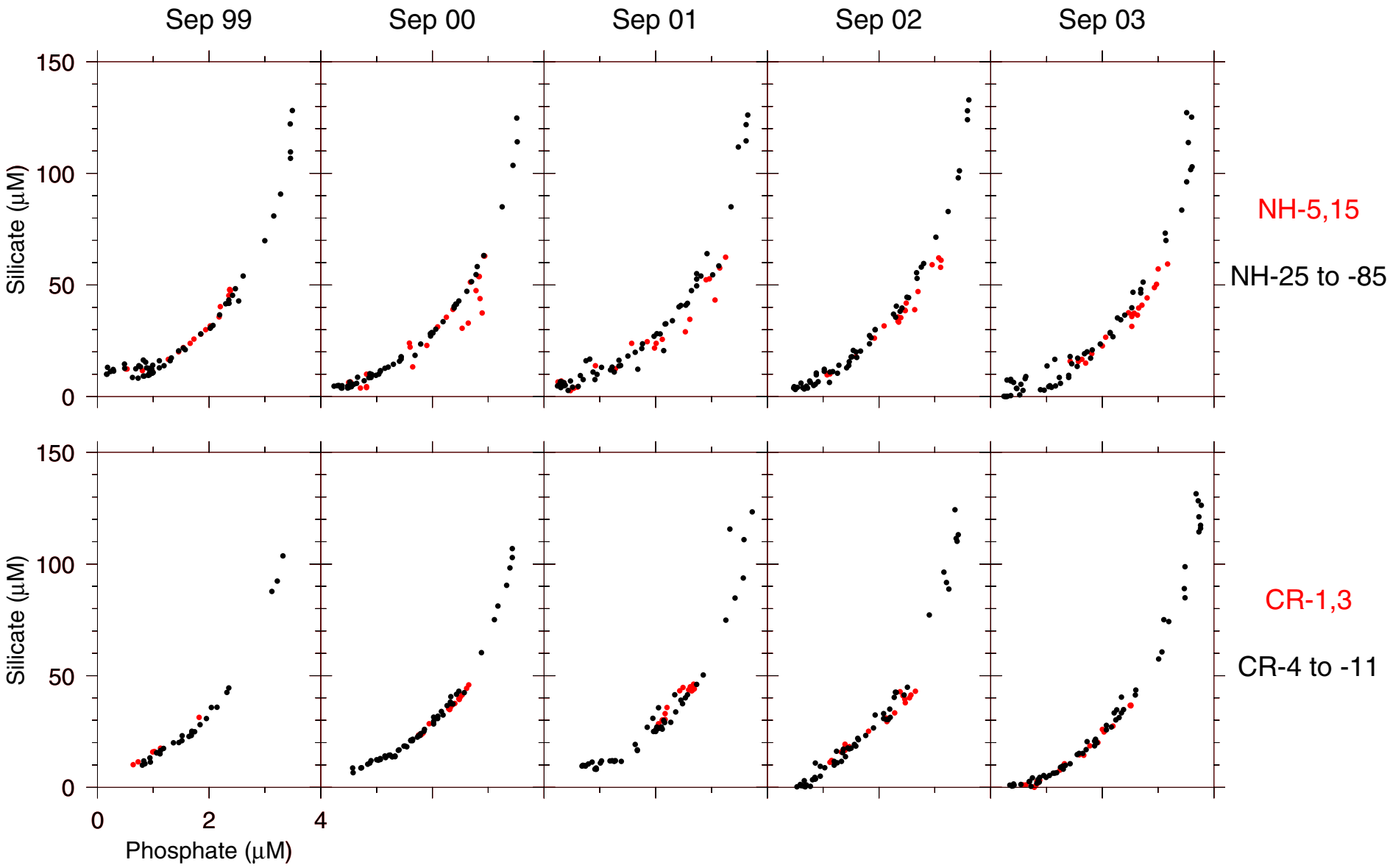

Figure 28. Silicate-phosphate relations for all rosette samples. Shelf stations are plotted in red.

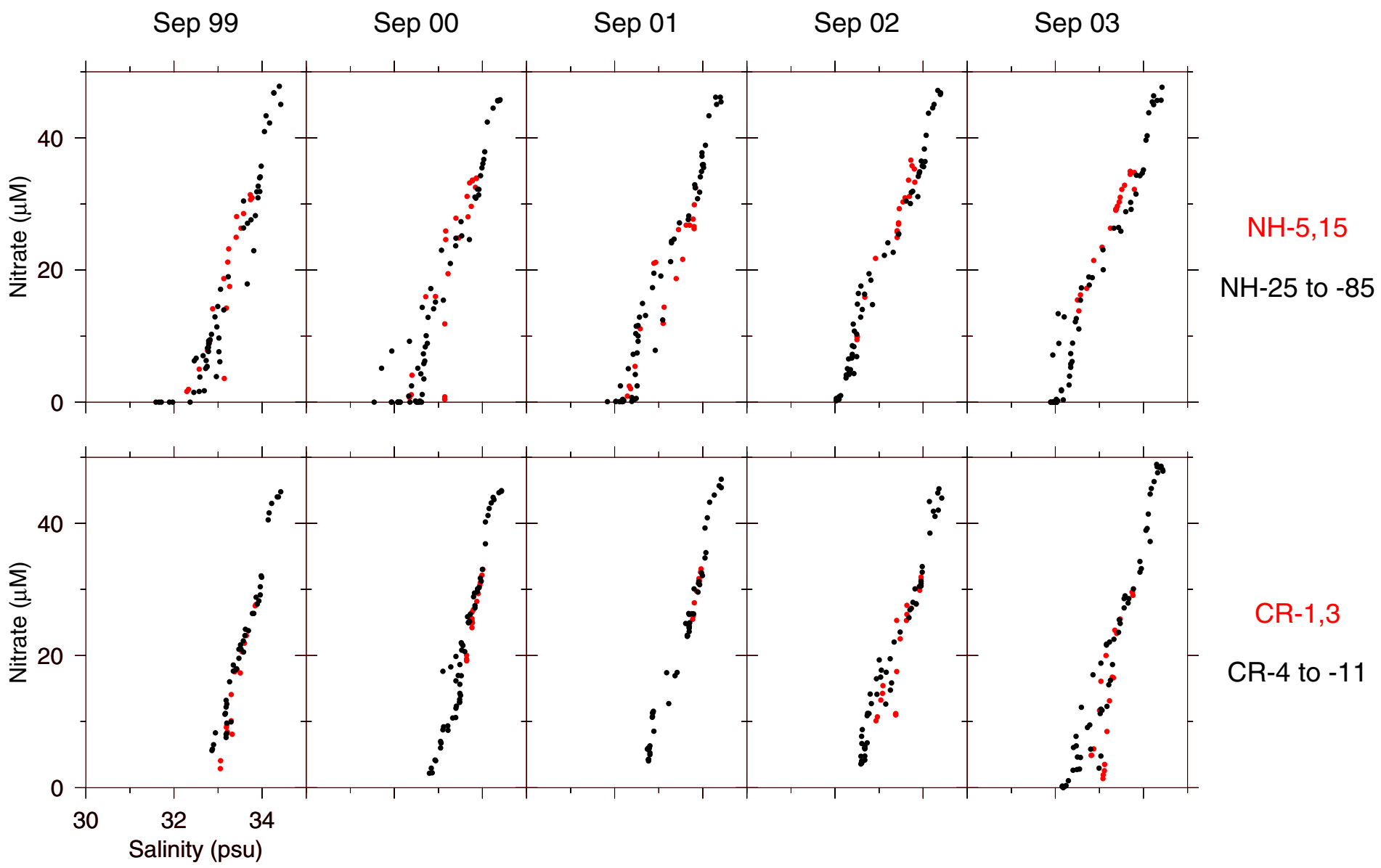

Figure 29. Nitrate-salinity relations. Shelf stations are plotted in red.

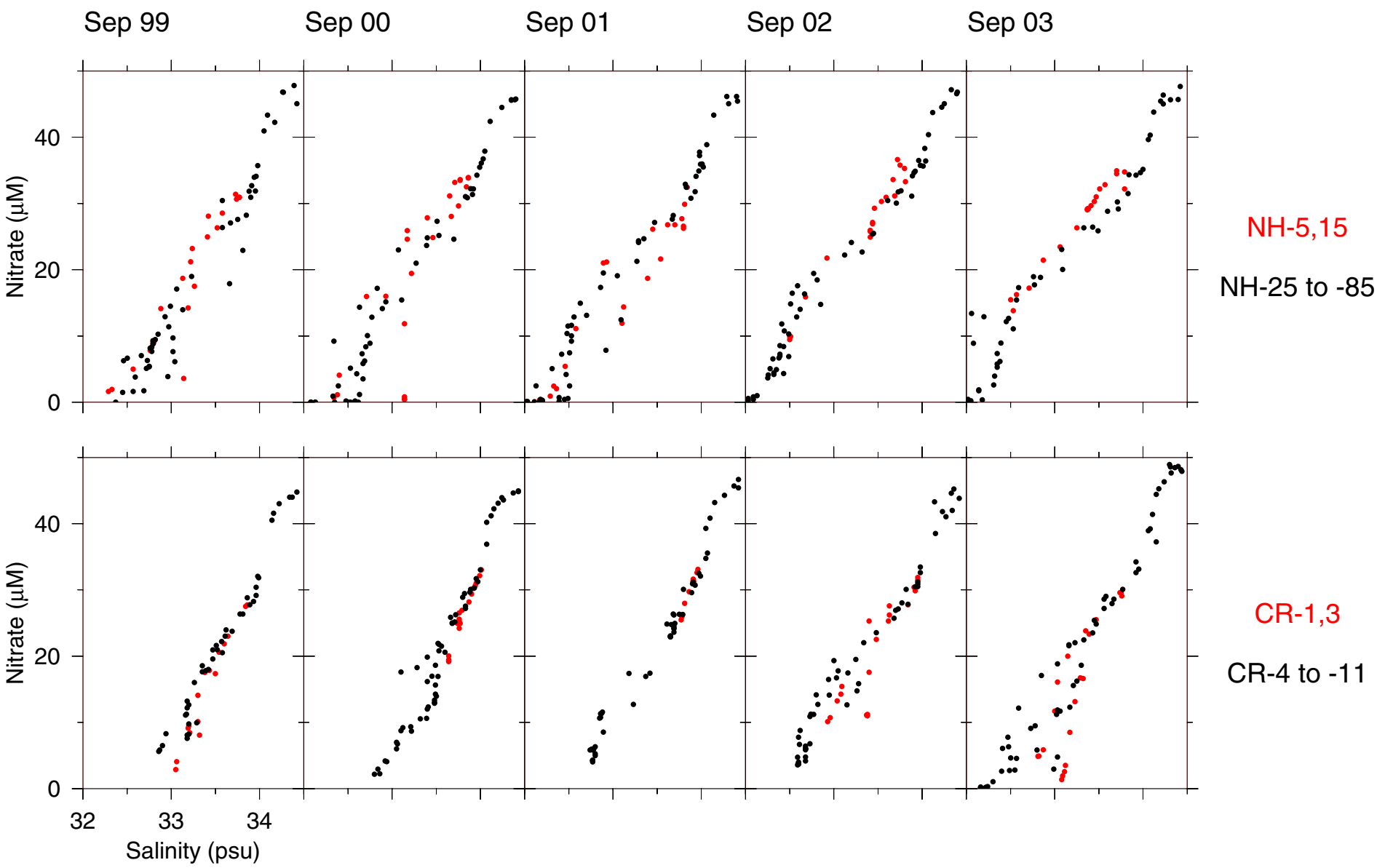

Figure 30. Nitrate-salinity relations for samples with salinities ≥ 32 psu. Shelf stations are plotted in red.

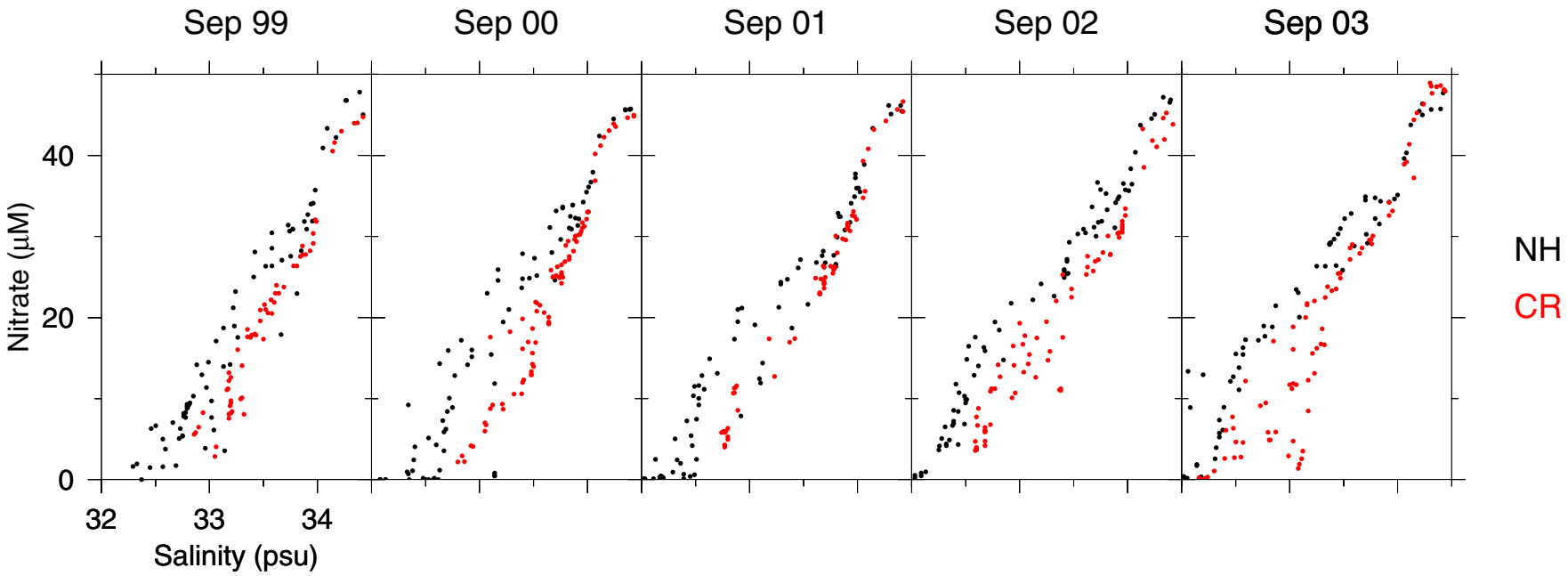

Figure 31. Nitrate-salinity relations for samples with salinities ≥ 32 psu: CR data (red) superimposed on NH data (black).

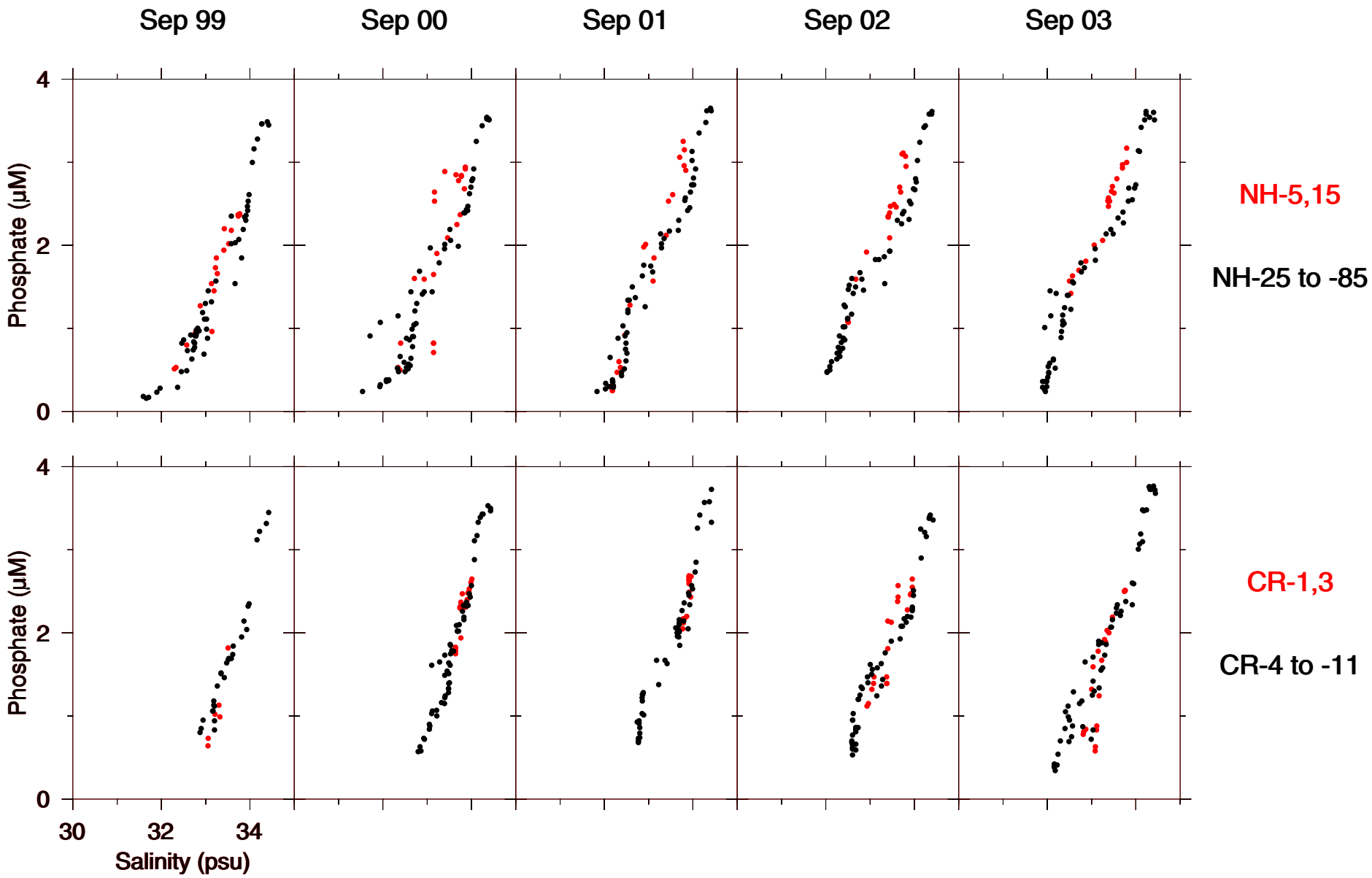

Figure 32. Phosphate-salinity relations. Shelf stations are plotted in red.

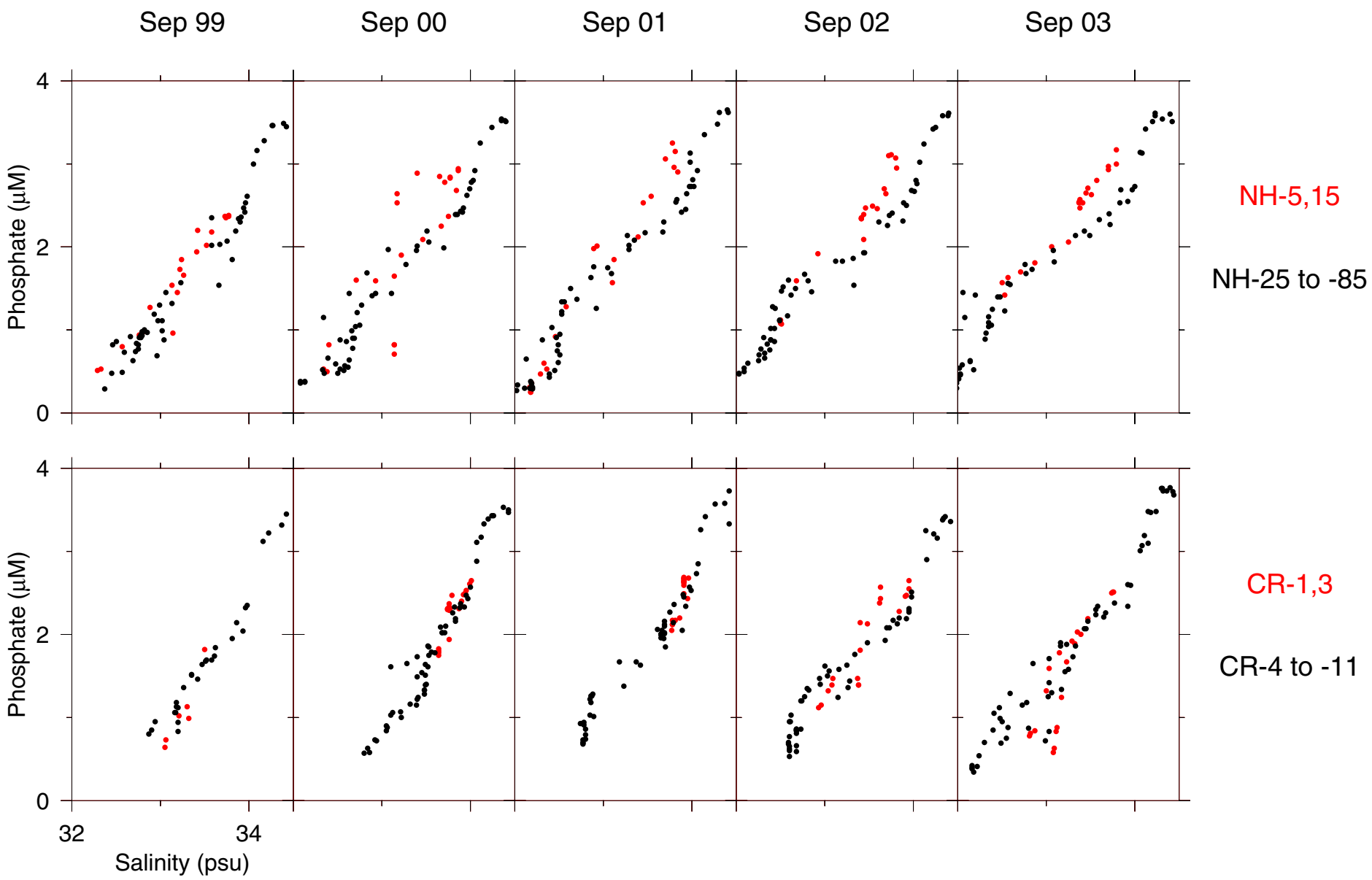

Figure 33. Phosphate-salinity relations for samples with salinities ≥ 32 psu. Shelf stations are plotted in red.

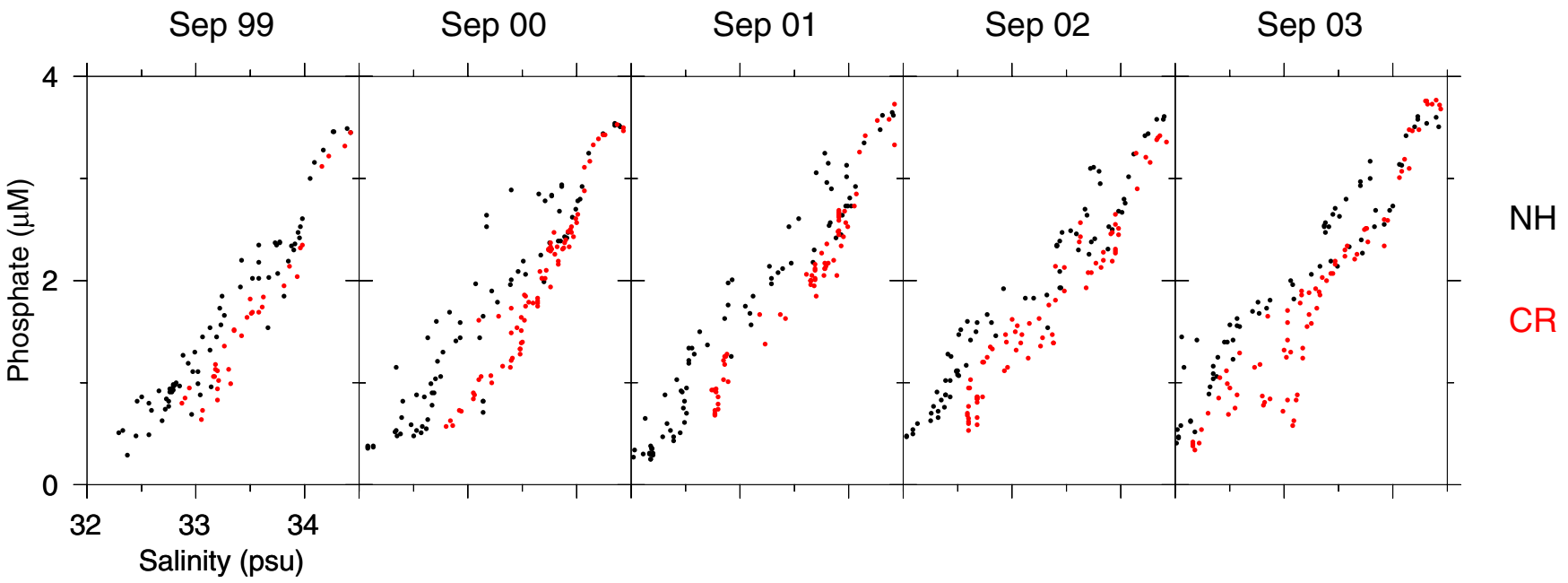

Figure 34. Phosphate-salinity relations for samples with salinities ≥ 32 psu: CR data (red) superimposed on NH data (black).

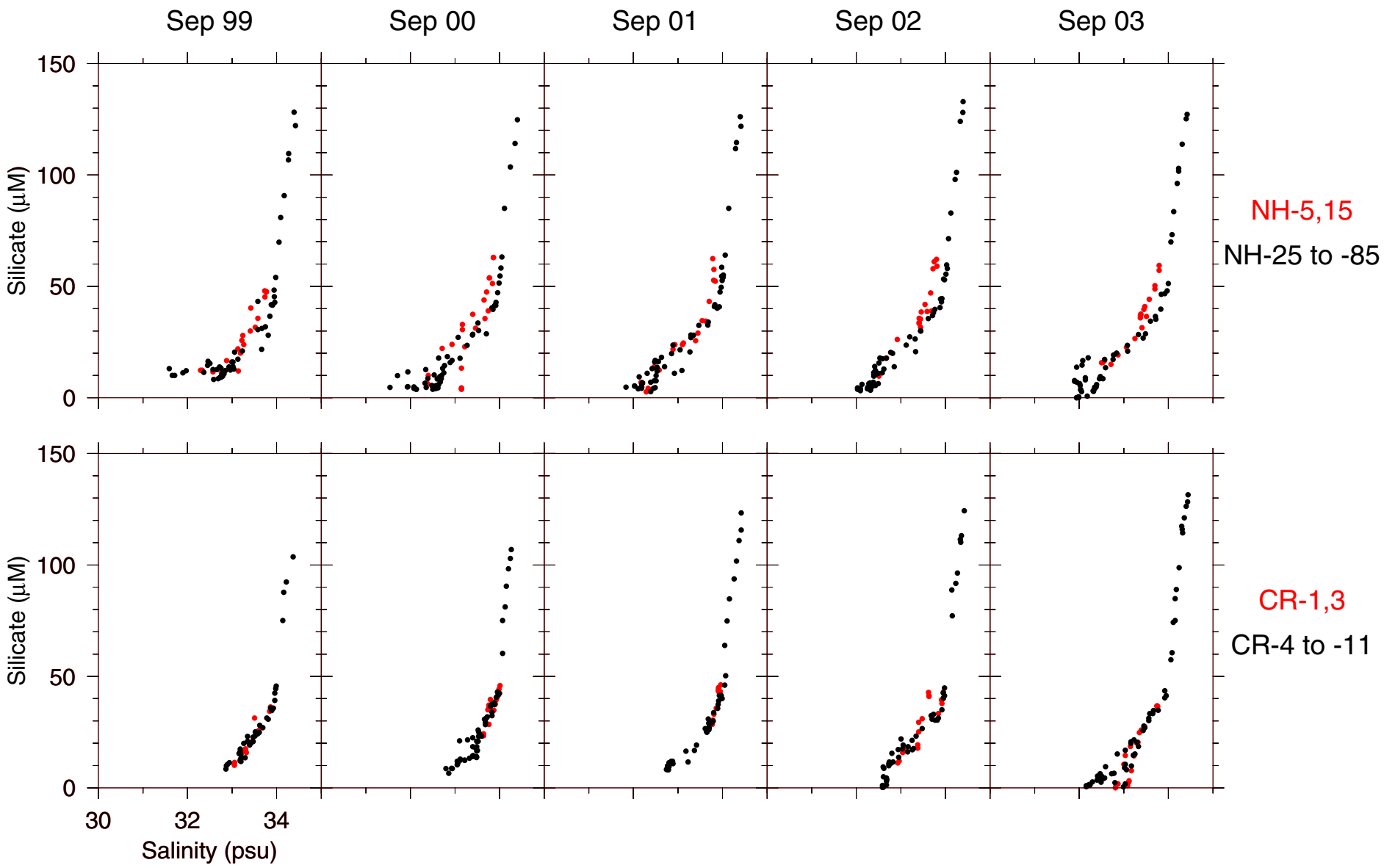

Figure 35. Silicate-salinity relations. Shelf stations are plotted in red.

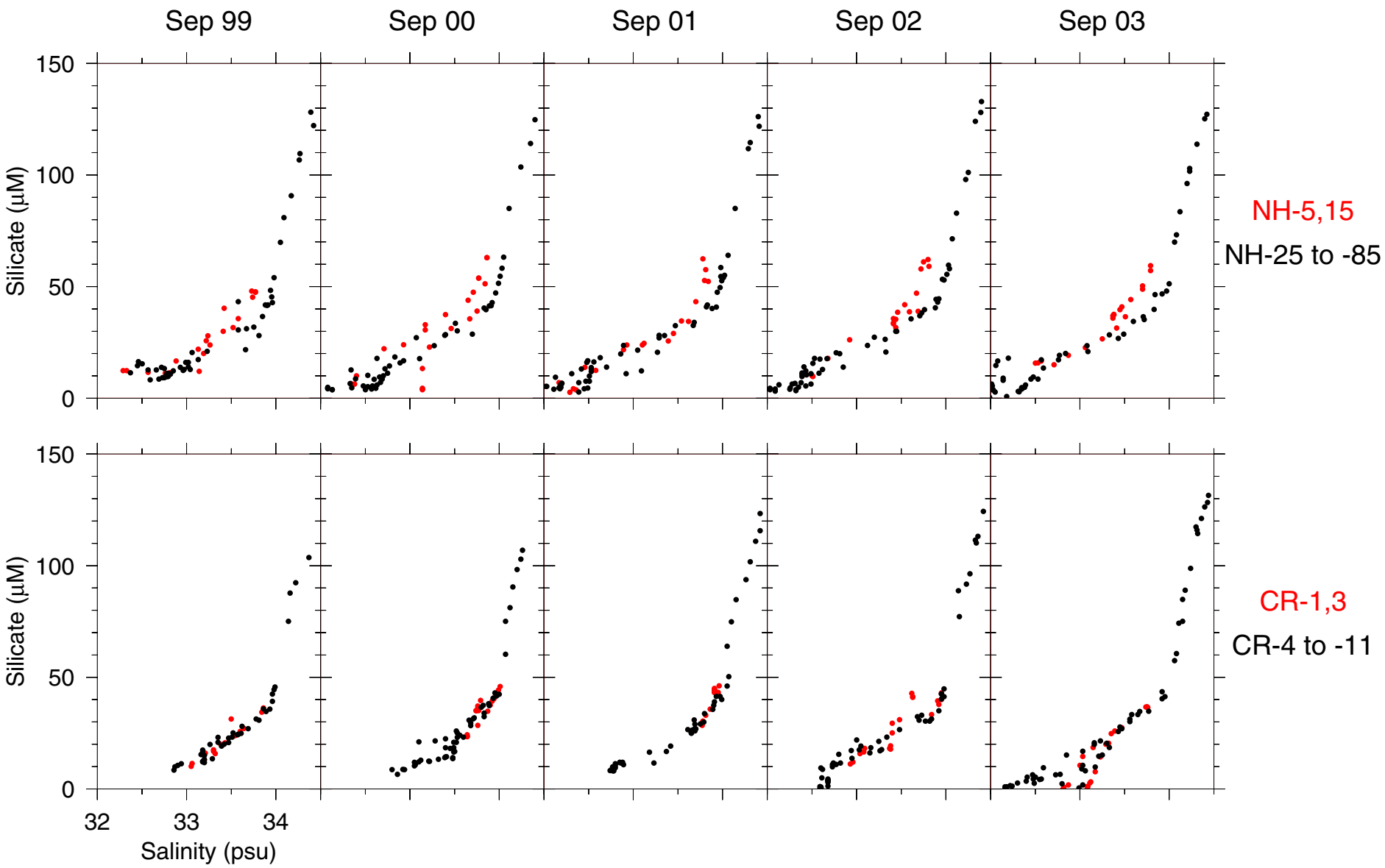

Figure 36. Silicate-salinity relations for samples with salinities ≥ 32 psu. Shelf stations are plotted in red.

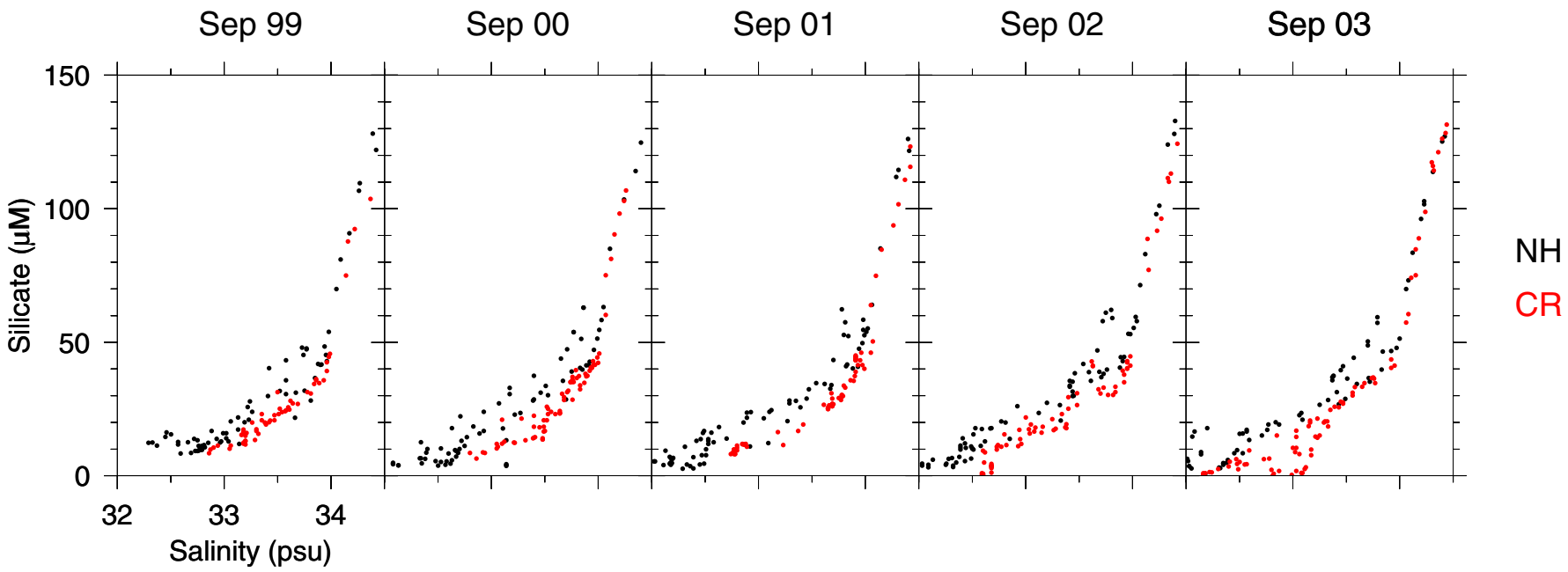

Figure 37. Silicate-salinity relations for rosette samples with salinities ≥ 32 psu: CR data (red) superimposed on NH data (black).